Computation of Invariant Tori

by

Kossi Delali Edoh

B.Sc.(Hons), Univ. of Cape Coast, 1986

Dip. in Education, Univ. of Cape Coast, 1986

THESIS SUBMITTED IN PARTIAL FULFILLMENT OF
THE REQUIREMENT FOR THE DEGREE OF
MASTER OF SCIENCE
in the Department
of
Mathematics and Statistics

SIMON FRASER UNIVERSITY

October 1991

Approval

Name: Kossi Delali Edoh

Degree: Master of Science (Mathematics)

Title of thesis: Computation of Invariant Tori

Examining Committee:

Chairman: *Dr. A.H. Lachlan*

Dr. R.D. Russell
Senior Supervisor

Dr. M. Trummer

Dr. A. Das

Dr. E. VanVleck
External Examiner
Department of Mathematics and Statistics
Simon Fraser University

Date Approved: October 1, 1991

PARTIAL COPYRIGHT LICENSE

I hereby grant to Simon Fraser University the right to lend my thesis, project or extended essay (the title of which is shown below) to users of the Simon Fraser University Library, and to make partial or single copies only for such users or in response to a request from the library of any other university, or other educational institution, on its own behalf or for one of its users. I further agree that permission for multiple copying of this work for scholarly purposes may be granted by me or the Dean of Graduate Studies. It is understood that copying or publication of this work for financial gain shall not be allowed without my written permission.

Title of Thesis/~~Project/Extended Essay~~

COMPUTATION OF INVARIANT TORI

Author:

(signature)

EDOH, KOSSI DELALI

(name)

OCT 25, 1991

(date)

Abstract

An important class of non-constant solutions of differential equations is periodic. In some cases a periodic solution can be written as the sum of a countable number of periodic functions each of whose periods is an integer combination of some base frequencies. The number p of base frequencies gives a p-periodic solution. Two-periodic solutions occur in both autonomous and non-autonomous systems. In this thesis we consider three methods for locating this behaviour. The first is a generalization of finite differences and uses the algorithm proposed by Kevrekidis which was later modified by van Veldhuizen. The second, similar to the first, uses the idea of the Hadamard graph transform. The third, the partial differential equation approach, solves a system of partial differential equations subject to periodic boundary conditions. The three methods are contrasted using simple dynamical systems. The Hadamard graph transform approach does very well on the van der Pol oscillator problem and the delayed logistic map but has some difficulties with the coupled oscillators problem. We also use computer graphics to illustrate dynamics on a two-torus.

Acknowledgements

I would like to take this chance to express my appreciation to Prof R. D. Russell for his excellent supervision on the preparation of this thesis and for helping me go through this program.

I would like to thank Dr M. Trummer, Dr P. Cahoon, L. Liu, M. Fankboner and S. Holmes who in one way or the other helped me during my studies here. Finally, my appreciation to the Department and the University as a whole for giving me the opportunity to study here.

Dedication

To my Parents.

Table of Contents

List of Tables

List of Figures

Introduction

Problems of dynamics have been with mankind for ages. The study of dynamic models has led to the theory of differential equations. There seems to be a fairly complete theory for linear ordinary differential equations, whereas much remains to be done in non-linear differential equations. Perhaps, the only known method developed so far is the use of perturbation methods for weakly nonlinear problems.

Poincaré showed (late 19 th century) that perturbation methods may not yield correct results in all cases, because the series used in such calculations diverge. He went on to relate analysis and geometry in his development of a qualitative approach to the study of differential equations. Some early workers in this area are Poincaré (1880, 1890, 1899), Birkhoff (1927) Andronov et al. (1937, 1966, 1971, 1973), Arnold (1973, 1978, 1982) and Smale (1967).

The solutions to dynamical systems lie frequently on a manifold (where a k-dimensional manifold M is a set of points that locally resembles R^k). One such important manifold is the torus. The main motivation for the computation of invariant circles and thus a torus is to use computer graphics to explain the geometry of the dynamics on the torus.

The purpose of this thesis is to compare three methods of computing an invariant torus for some simple dynamical systems. Apart from these three methods we mention briefly others by Thoulouze -Pratt and Jean [TPJM], Chan [CHA] and Parker [PTCL]. The process described in [TPJM] may fail for problems with an almost rational rotation numbers. Chan based one of his methods on the collocation approximation of the invariant curve and in the process the curve was parameterised such that the circle map becomes a rigid rotation. The process described in [PTCL] using the spectral balance approach is for equations with two or more periodic forcing terms of incommensurate frequencies. It involves solving a linear system of equations with columns whose orthogonality depends on the discretization of time.

There were some early works like the direct iteration of the map which was generally

used for computing invariant circles in [ACHM]. This method fails when the invariant circles are repelling. Also Iooss G, Arneeodo A, Coullet P, and Tresser C. [IACT] tried to obtain an explicit analytic expression of the invariant circles for a general 2-dimensional diffeomorphisms but it turned out to be too complicated. The work by Levison [LEN] gives a good introduction to the existence theory for invariant curves. His work was followed by that of Hale [HJK].

In chapter one, basic terms used in the qualitative theory of dynamical system are given with emphasis on their definitions and their interpretation in the physical world. Chapter two gives an insight into HOOPS graphics system which was used to draw the diagrams in this thesis. In chapter three we discuss the methods of Kevrekidis, van Veldhuizen and the Hadamard graph transform approach. The three methods use a polygonal approximation to the invariant curve that is to be computed. Chapter four discusses the pde approach. This involves solving a system of partial differential equations subject to periodic boundary conditions. In Chapter five we compared the results obtained using the Hadamard graph transform approach to that obtained by van Veldhuizen and the pde approach. Chapter six gives a brief discussion of the methods of Chan, Thoulouze Pratt and Jean, the spectral balance method and finally some conclusions are given in chapter 7.

Chapter 1

Some basic concepts in the theory of ode's and dynamical systems

1.1 Autonomous and Non-autonomous systems

The state equation

$$\dot{x} = f(x), \qquad x(t_0) = x_0, \tag{1.1.1}$$

where $f : R^n \longrightarrow R^n$ (vector field) is called an n^{th} - order continuous autonomous dynamical system. Let $\phi_t(x_0)$ denote the solution to (1.1.1) at time t and satisfying the initial condition such that the solution at time $t = t_0$ is x_0 ($\phi_{t_0}(x_0) = x_0$) and also satisfying the condition $\phi_{t_1+t_2} = \phi_{t_1} o \phi_{t_2}$. The trajectory through the point x_0 is the set $\{\phi_t(x_0) : -\infty < t < \infty\}$. The one-parameter family of mappings $\phi_t : R^n \longrightarrow R^n$ is called the flow.

In the non-autonomous case, we have

$$\dot{x} = f(x,t), \qquad x(t_0) = x_0, \tag{1.1.2}$$

and the solution is $\phi_t(x_0, t_0)$. We assume that for any t, ϕ_t, and $\phi_t(., t_0)$ are diffeomorphisms. A smooth map $\phi : x \longrightarrow y$ is a diffeomorphism if it is invertible and if the inverse map $\phi^{-1} : y \longrightarrow x$ is also smooth. A map $f : V \longrightarrow R^p$ is smooth if it possesses continuous

derivatives of all orders, where $V \subset R^m$ is an open set.

1.2 Poincaré map

In this section instead of considering the bifurcation problem from a periodic solution to an invariant tori in an ordinary differential system, we will reduce it to the simpler bifurcation problem from a fixed point to an invariant circle in 2-dimensional diffeomorphic maps. This is done with the idea of the Poincaré map. A periodic solution corresponds to a fixed point x^* of the Poincaré map and an invariant torus corresponds to an invariant circle of the associated Poincaré map. Bifurcation to an invariant circle from a fixed point is only one of the many types of dynamical behaviours that have been observed [GIMC].

An n^{th} order non-autonomous system with minimum period T can be transformed into an $(n+1)^{th}$ order autonomous system in the cylindrical state space R^n x S^1 where

$$S^1 := [0, 2\pi).$$

Using the transformation $\theta := 2\pi t/T$, equation (1.1.2) becomes

$$\dot{x} = f(x, \theta T/2\pi), \qquad x(t_0) = x_0.$$

$$\dot{\theta} = 2\pi/T, \qquad \theta(t_0) = 2\pi t_0/T. \tag{1.2.3}$$

Considering the hyperplane

$$\sum := \{(x, \theta) \in R^n \times S^1 : \theta = \theta_0\} \tag{1.2.4}$$

then for every time T the trajectory

$$\begin{bmatrix} x(t) \\ \theta(t) \end{bmatrix} = \begin{bmatrix} \theta_t(x_0, t_0) \\ 2\pi t/T (mod 2\pi) \end{bmatrix}$$

intersects (1.2.4).

The map

$$P_N : \sum \longrightarrow \sum (R^n \longrightarrow R^n)$$

defined by $P_N(x) := \phi_{t_0+T}(x, t_0)$ is called the Poincaré map. The set

$$\{P_N^K(x) = \phi_{t_0+kT}(x, t_0) \quad k = 1, 2, ...\} \tag{1.2.5}$$

is called the corresponding orbit. Since ϕ_t is a diffeomorphism for any fixed t, it follows that $P_N(x)$ is also a diffeomorphism [PTCL].

For the Poincaré map of an n^{th} order autonomous system, denoted P_A, the Poincaré map corresponding to a limit cycle Γ (where a limit cycle is an isolated periodic solution of an autonomous system and where an autonomous periodic solution $\phi_t(x^*)$ is such that $\phi_t(x^*) = \phi_{t+T}(x^*)$ for some minimun periodic T > 0) is as follows:

Let $x^* \in \Gamma$ and $\sum$ be an (n- 1)- dimensional hyperplane transversal to Γ at x^* with T the minimum period of the limit cycle. Two manifolds, $Ma_1 \subset R^n$ and $Ma_2 \subset R^n$, are said to be transversal if for each $x \in Ma_1 \bigcap Ma_2$, $T_x(Ma_1) + T_x(Ma_2)$ span R^n where $T_x(M)$ is the tangent space of M at x. Since ϕ_t is continuous with respect to the initial conditions, the trajectories starting on $\sum$ in a small neighborhood of x^* will intersect $\sum$ in the vicinity of x^* in approximately T seconds. The Poincaré map P_A consisting of ϕ_t and $\sum$ defines a mapping $P_A : U \longrightarrow V$ where $x^* \in U \subset \sum$ and $P_A(x^*) \in V \subset \sum$.

Some remarks:

- P_A is defined locally in the neighborhood of x^*. In this case it is guaranteed that the trajectory emanating from any point on $\sum$ will intersect $\sum$.
- In Euclidean state space, $\phi_t(x)$ must pass through $\sum$ at least once before returning to V.
- P_A is a diffeomorphism. The proof of this is in [PTCL].
- P_A can be determined if one has a knowledge of the position of the limit cycle.

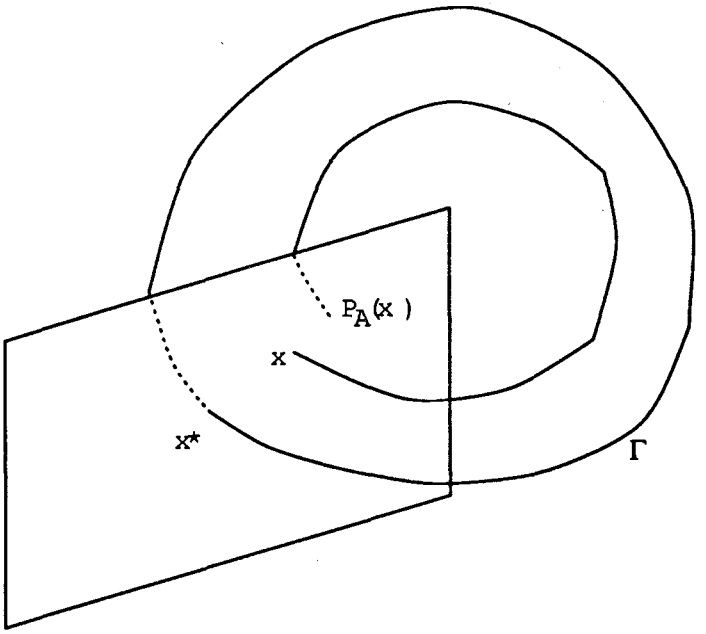

Fig. 1.1 : The Poincaré map P_A for a third-order autonomous system with limit cycle Γ.

1.3 Stability of a fixed point

An invariant circle may be spawned as a fixed point loses stability through a Hopf bifurcation (Hopf bifurcation is described in section 1.4). In this section we look at the stability of a fixed point.

The set of all eigenvalues of a linear transformation $G : R^n \longrightarrow R^n$, $\sigma(G)$, is called the spectrum of G. Let x^* be a fixed point of a Poincaré map P and T be the period of the system. In the non-autonomous system

$$P_N(x^*) := \phi_T(x^*, t_0) \tag{1.3.6}$$

and

$$\Phi_T(x^*, t_0) =: DP_N(x^*) = D_x\phi_T(x^*, t_0) \tag{1.3.7}$$

where $\Phi_t(x_0, t_0)$ is called the fundamental solution matrix of (1.3.10). Thus

$$\sigma(\Phi_T(x^*, t_0)) = \sigma(DP_N(x*)).$$

In the autonomous case

$$\Phi_T(x^*) = D_x(P(x^*)) \tag{1.3.8}$$

and

$$\sigma(\Phi_T(x^*)) = \sigma((DP(x^*)) \ \cup \{1\}. \tag{1.3.9}$$

The term $\Phi_t(x_0, t_0)$ is determined as follows:

From (1.1.2) we get

$$\dot{\phi}_t(x_0, t_0) = f(\phi_t(x_0, t_0), t), \qquad \phi_{t_0}(x_0, t_0) = x_0, \tag{1.3.10}$$

and taking the derivative of (1.3.10) with respect to x at x_0 we get

$$D_{x_0}\dot{\phi}_t(x_0, t_0) := D_x f(\phi_t(x_0, t_0), t) D_{x_0}\phi_t(x_0, t_0), \qquad D_{x_0}\phi(x_0, t_0) = I.$$

This can be written as

$$\dot{\Phi}_t(x_0, t_0) = D_x f(\phi_t(x_0, t_0)\Phi_t(x_0, t_0), \qquad \Phi_{t_0}(x_0, t_0) = I, \tag{1.3.11}$$

and is called the variational equation of (1.3.10). For the autonomous system, the variational equation is given by

$$\dot{\Phi}_t(x_0) = D_x f(\phi_t(x_0))\Phi_t(x_0), \qquad \Phi_{t_0}(x_0) = I. \tag{1.3.12}$$

From (1.3.11) and (1.3.12) we get $\Phi_t(x_0, t_0)$ and $\Phi_t(x_0)$ respectively.

Let the eigenvalues of $DP(x^*)$, called the characteristic multipliers, be given by $m_i \ \ i = 1, ..., n$. Then the fixed point is asymptotically stable if $|m_i| < 1$ for all i and is non-stable if for some i, $|m_i| < 1$ and for some i, $|m_i| > 1$. It is unstable if $|m_i| > 1$ for all i. The fixed point is hyperbolic if $|m_i| \neq 1$ for all i. It is then said to be generic and structurally stable. The characteristic multipliers (eigenvalues) in the autonomous case are independent of the position of the cross-section $\sum$ and in the non-autonomous case they are independent of the choice of t_0. On the other hand, the eigenvectors depend on the position of $\sum$ in the autonomous case and on t_0 in the non-autonomous case.

1.4 Normal forms

Here we introduce the concept of Hopf bifurcation and give a series of transformations that reduce our map to a simple form called the normal form to which the Hopf bifurcation theorem is applied. Consider the map

$$F_\lambda \begin{pmatrix} x \\ y \end{pmatrix} = (\lambda + \beta(x^2+y^2)) \begin{pmatrix} cos\alpha & -sin\alpha \\ sin\alpha & cos\alpha \end{pmatrix} \begin{pmatrix} x \\ y \end{pmatrix}. \tag{1.4.13}$$

In polar coordinates this family of maps can be written as

$$r_1 = \lambda r + \beta r^3$$

$$\theta_1 = \theta + \alpha. \tag{1.4.14}$$

This map has an invariant circle given by $r = \sqrt{(1-\lambda)/\beta}$ provided $(1-\lambda)/\beta > 0$. When

$$\beta < 0 \text{ and } \lambda > 1,$$

the invariant curve is attracting and when

$$\beta > 0 \text{ and } \lambda < 1,$$

the invariant curve is repelling. The eigenvalues of the system (1.4.13) at the fixed point (0,0) are $-\lambda$ and λ. And at $\lambda = 1$ the eigenvalues cross the unit circle. When $\lambda < 1$ the fixed point is attracting and when $\lambda > 1$ the fixed point is repelling. Therefore, as an attracting fixed point becomes repelling, an invariant circle is created. The bifurcation which occurs at $\lambda = 1$ is called Hopf bifurcation. In general, using Taylor series, any nonlinear mapping F_μ which fixes the origin ($F(0) = 0$) may be put in the form

$$x_1 = \alpha x - \beta y + O(2)$$

$$y_1 = \beta x + \alpha y + O(2), \tag{1.4.15}$$

where the expression O(2) indicates terms of degree two or more, i.e.

$$\alpha_1 x^2 + \alpha_2 xy + \alpha_3 y^3 + \dots .$$

Letting $\mu = \alpha + i\beta$ and z = x + iy, then (1.4.15) becomes

$$z_1 = x_1 + iy_1 = \mu z + 0(2). \tag{1.4.16}$$

By a judicious choice of conjugacy near the origin, we can eliminate some higher order terms (using a nonlinear coordinate transformation).

Definition ♣ Let $f : A \longrightarrow A$ and $g : B \longrightarrow B$ be two maps. f and g are said to be topologically conjugate if there exists a homeomorphism $h : A \longrightarrow B$ such that,

h o f = g o h. The homeomorphism h is called a topological conjugacy.♣

Theorem 1.31

♣ Suppose $F_\mu(z) = \mu z + O(5)$, where μ is not a k^{th} root of unity for k=1,...,5. Then there is a neighborhood U of 0 and a diffeomorphism h on U such that the map $h^{-1}oF_\mu oh$ assumes the form

$$z_1 = \mu z + \beta(\mu)z^2\bar{z} + O(5).\clubsuit \tag{1.4.17}$$

In polar coordinates 1.4.17 becomes

$$r_1 = |\mu|r + \beta(\mu)r^3 + O(5)$$

$$\theta_1 = \theta + \alpha(\mu) + \gamma(\mu)r^2 + O(5), \tag{1.4.18}$$

where $\mu = |\mu|e^{i\alpha}$ and β, γ are constants. O(5) are terms of 5^{th} and higher powers of r. Equation (1.4.17) and (1.4.18) are in normal form. For the proof we use the following propositions which form the general procedure of reducing a map to a normal form.

Proposition 1

♣ Let F_μ be a map of the form

$$z_1 = \mu z + \alpha_1 z^2 + \alpha_2 z\bar{z} + \alpha_3\bar{z}^2 + O(3), \tag{1.4.19}$$

where $\mu \neq 0$. Then there exists a neighborhood U_1 of 0 and a diffeomorphism $L_1 : U_1 \longrightarrow R^2$ such that $L_1^{-1}oF_\mu oL_1$ assumes the form G_μ given by

$$z_1 = \mu z + O(3),$$

provided μ is not a k^{th} root of unity where k=1 or 3. ♣

Proposition 1 eliminates the O(2) terms in the map (1.4.19).

Proposition 2

♣ Let G_μ be a map of the form

$$z_1 = \mu z + \beta_1 z^3 + \beta_2 z^2 \bar{z} + \beta_3 z \bar{z}^2 + \beta_4 \bar{z}^3 + O(4) \tag{1.4.20}$$

where $\mu \neq 0$. Then there exists a neighborhood U_2 of 0 and a diffeomorphism $L_2 : U_2 \longrightarrow R^2$ such that $L_2^{-1} o G_\mu o L_2$ assumes the form H_μ given by

$$z_1 = \mu z + \beta_2 z^2 \bar{z} + O(4)$$

provided μ is not a k^{th} root of unity for k=2 or 4. ♣.

Proposition 2 eliminates some of the O(3) terms in the map (1.4.20).

Proposition 3

♣ Let H_μ be a map of the form

$$z_1 = \mu z + \beta_2 z^2 \hat{z} + O(4) \tag{1.4.21}$$

where $\mu \neq 0$. Then there exists a neighborhood U_3 of 0 and a diffeomorphism $L_3 : U_3 \longrightarrow R^2$ such that $L_3^{-1} o H_\mu o L_3$ assumes the form

$$z_1 = \mu z + \beta_2 z^2 \bar{z} + O(5)$$

provided μ is not a k^{th} root of unity for k=3 or 5. ♣

Remark:

Suppose

$$F : R^2 \longrightarrow R^2$$

satisfies F(0) = 0 and DF(0) has an eigenvalue μ where $\mu^k = 1, \quad k > 3$. Then a sequence of transformations from propositions 1,2, and 3 allows us to put F in the form

$$z_1 = \mu z + \beta_1 |z|^2 z + \beta_2 |z|^4 + ... + \beta_l |z|^{2l} z + \gamma \hat{z}^{k-1} + O(k) \tag{1.4.22}$$

where $\beta_1, \beta_2, ...\beta_l, \gamma$ are constants and l is the fractional part of (k-2)/2. Equation (1.4.22) is the generalized normal form. For the complete proof see [DRL]. In the case of a flow, the idea of successive coordinate transformations to simplify the analytic expression of a general problem forms the basis of the Kolmogorov-Arnold-Moses (KAM) theory for studying quasiperiodic phenomena. To get the normal form for flows see [GJHP].

♣ Theorem 1.2 **(Hopf bifurcations for maps)**

Let $f_\mu : R^2 \longrightarrow R^2$ be a one-parameter family of mappings which has a smooth family of fixed points x(μ) at which the eigenvalues are complex conjugates $\lambda(\mu), \bar{\lambda}(\mu)$. Assume

$$|\lambda(\mu_0)| = 1, \qquad \text{but } \lambda^j(\mu_0) \neq 1, \qquad \text{for } j = 1, 2, 3, 4 \tag{1.4.23}$$

$$\frac{d}{d\mu}(|\lambda(\mu)|) = d \neq 0. \tag{1.4.24}$$

Then there is a smooth change of coordinates h so that the expression of $hf_\mu h^{-1}$ in polar coordinates has the form

$$hf_\mu h^{-1}(r, \theta) = (r(1 + d(\mu - \mu_0) + ar^2), \theta + c + br^2) + \text{higher order terms.} \tag{1.4.25}$$

(note: λ complex and (1.4.24) imply $|arg(\lambda)|$ = c and d are nonzero.) If, in addition,

$$a \neq 0 \tag{1.4.26}$$

then there is a two-dimensional surface $\sum$ (not necessarily infinitely differentiable) in R^2xR having quadratic tangency with the plane R^2x $\{\mu_0\}$ which is invariant for f. If $\sum \cap (R^2 \text{x} \{\mu\})$ is larger than a point, then it is a simple closed curve ♣ .

The signs of a and d determine the direction and stability of the periodic bifurcating orbit, while c and b give information on rotation numbers. The equation (1.4.25) is the normal form. If $\frac{d}{d\mu}|\lambda(\mu)| > 0$ when $\lambda = 0$ then the eigenvalues cross from the inside to the outside of the unit circle as μ increases.

The centre manifold theorem enables us to extend the 2-dimensional Hopf bifurcation to higher dimension. It reduces an infinite dimensional problem to a finite dimensional one.

Theorem 1.3 (Centre Manifold Theorem for a map)

♣ Let h be a mapping of a neighborhood of zero in a Banach space B into B. Assume h is C^{k+1} and h(0) = 0. Further assume that the spectrum of $h'(0)$ is contained in the unit circle and the spectrum splits into two parts where one pair is on the unit circle and the remaining part is at a non-zero distance from the circle. Let Y denote the generalized eigenspace of $h'(0)$ belonging to the part of the spectrum on the unit circle. Assume that Y has dimension $d < \infty$.

Then there exists a neighbourhood V of 0 in B and a C^k submanifold M of V of dimension d, passing through 0 and tangent to Y at 0 such that

(1) Local invariance: If $x \in M$ and $h(x) \in V$, then $h(x) \in M$.

(2) Local attractivity: If $h^n(x) \in V$ for all n=0,1,2,... Then $H(h^n(x), M) \longrightarrow 0$ as $n \longrightarrow \infty$, where H is the Hausdorff distance. ♣

Definition: ♣ A subset S of a normed linear space E is called a submanifold of E if S has the following property: For each $x \in$ S, there is a neighborhood U of x in E and a diffeomorphism $\psi : U \longrightarrow V$, where V is an open set in E such that

$$\psi(S \cap U) = L \cap V$$

where L is some affine subspace of E. ψ is called a chart of S. ♣

1.5 Rotation Numbers

The dynamics on the torus is determined by the rotation number of the associated invariant circle. In this section we give the definition of rotation number and then its properties.

Let us denote an invariant circle by S^1 and consider the diffeomorphism

$$f : S^1 \longrightarrow S^1.$$

If f is an orientation preserving diffeomorphism, then for $x < y < z$,

$$f(x) < f(y) < f(z). \tag{1.5.27}$$

The diffeomorphism f can be "lifted" to a map $F : R \longrightarrow R$ which covers f via the covering projection

$$\sigma : R \longrightarrow S^1$$

defined by

$$\sigma(t) = exp(2\pi it).$$

It is clear that σ maps R around S^1.

Definition

♣$F : R \longrightarrow R$ is a lift of $f : S^1 \longrightarrow S^1$ if

$$\sigma oF = fo\sigma.\clubsuit \tag{1.5.28}$$

There are many lifts for a given map $f : S^1 \longrightarrow S^1$ and any two lifts of f differ only by translation (integer) [NIN]. If F is the lift of f then we must have $F'(x) > 0$ so that F is increasing and furthermore, $F(x+1) = F(x)+1$ or in general $F(x+k) = F(x)+k$ for any integer k.

Definition

♣ The rotation number of f, $\rho_y(f)$, is the fractional part of $\rho_0(F)$ for any lift F of f. That is, $\rho(f)$ is the unique number in [0,1) such that $\rho_0(F) - \rho_y(f)$ is an integer where

$$\rho_0(F) = lim_{n\longrightarrow\infty}\frac{|F^n(y)|}{n}. \tag{1.5.29}$$

Second definition

♣ We pick an arbitrary $x \in S^1$ and partition S^1 into two arcs $I_0 = [x, f(x))$ and $I_1 = [f(x), x)$. For any point $y \in S^1$, we define the rotation number

$$\rho_y(f) = \lim_{n\to\infty} 1/n[Cardinality\ \{f^i(y)|0 < i < n\ and\ f^i(y) \in I_0\}]. \tag{1.5.30}$$

Intuitively, $\rho_y(f)$ is the asymptotic proportion of the points on the trajectory which lie on I_0.

Some properties of $\rho_y(f)$ are:

- $\rho_y(f)$ exists and is independent of y.
- $\rho_y(f)$ is rational if and only if f has a periodic orbit.
- If the conditions of the Hopf bifurcation theorem for diffeomorphisms are satisfied then $\rho_y(f_\lambda)$ is a continuous function of the variable λ. [IOG]

The inverse of the rotation number indicates how many time intervals of length T (the period) are necessary to map a point x_0 on the invariant curve to itself by using it as an initial vector for the differential equation at time t=0.

1.6 Dynamics on the torus

Possible location of invariant tori

Consider the system

$$\dot{X} = F(X, \mu), \tag{1.6.31}$$

where $\mu = (\mu_1, \mu_2, ...,)$ are parameters and $X \in R^n$, $F : R^n \times R^n \longrightarrow R^n$. Let us adjoin the equation

$$\dot{\theta} = \omega \tag{1.6.32}$$

where ω is constant dependent on T and $\theta \in T$ a circle of circumference $2\pi/\omega$ to the periodic system of (1.6.31). The system (1.6.31) - (1.6.32) is defined in the phase space R^nxT and a periodic orbit of (1.6.31) becomes an invariant torus of (1.6.31)-(1.6.32). If (1.6.31) displays a period-doubling cascade as we vary μ suitably, (1.6.31)-(1.6.32) will exhibit a corresponding sequence of period doublings of invariant tori.

Now consider (1.6.31) and (1.6.32) coupled together by

$$\dot{X} = F(X, \mu) + \epsilon f(X, \theta)$$

$$\dot{\theta} = \omega + \epsilon g(X, \theta) \tag{1.6.33}$$

where $\epsilon > 0$ as a parameter. For sufficiently small ϵ the invariant tori of (1.6.31) and (1.6.32) can still persist when it has a normal hyperbolicity.

Also some parameters may introduce frequency lockings which is the occurance of periodic orbits on the tori. As the parameter ϵ increases the tori may begin to deform. This situation was observed for example in the ODE

$$\frac{d^3x}{dt^3} + \eta\frac{d^2x}{dt^2} + \mu\frac{dx}{dt} + \lambda x = x^2 + \epsilon\, cos(2\pi t)$$

by Arneodo, Coullet and Spiegel [ASC].

Chapter 2

Computer Graphics

2.1 Computer Graphics

Computer graphics is probably the most versatile and most powerful means of communication between the computer and the human being. The value of a picture as a means for communicating information quickly and accurately has long been recognised. As the ancient Chinese proverb goes "a picture is worth a thousand words" helps to explain the use of computer graphics in academic life. Computer graphics today is largely interactive, involving the technology of using computer-driven displays to control the contents, structure and appearance of objects. Computer graphics can be used in various aspects of our life and some of which is as follows:

- Computer aided design (CAD) in the manufacture of wireframe drawings can be displayed on a video screen to test the appearance of body shapes, e.g. automobiles, airplanes etc.
- Architectural design for room arrangement, door and window placement, or the location of various facilities.
- Educational applications utilize computer graphics in classroom demonstrations, computer generated exams, and self-study programs.

Computer graphics is an integral part of many people's life. The merging of analysis and geometry in dynamical systems (Poincaré) has created a new area of application for computer graphics. Many software systems have been developed to assist in the study of dynamical systems. e.g. DYNPAQ, KAOS, CHAOS, AUTO, DSTOOL and so on.

Hoops Graphics System

Hierarchical Object Oriented Plotting System (HOOPS) from Ithaca software is a system for creating interactive graphics applications. Its database is organised as a tree-shaped hierarchy which is similar to a file directory tree in the unix systems. The database has units which are called segments, and the segment's data consists of geometrical primitives, cameras, lights, rendering and modelling attributes, and application-specific information. The segments have a hierarchical structure organisation which makes them easy to manipulate.

- Suppose one wants to display the objects

  car1 denoted by segA,

  car2 denoted by segB,

  tires denoted by segC,

  then one begins by declaring a HOOPS picture segment that will define segA, segB, and segC. One way of doing this is

- one creates ?Include/Library/tires which includes a database segment that contains the graphical definition of tires.

- one creates the segA.

- one creates the segB.

- one includes segC in segB, and segA.

A 'C' code for what is described above

- Open_Segment("?Picture");
- Open_Segment("tires");
- Make_tires();
- Close_Segment();
- Open_Segment("segA");
- Make_part_car1();
- Include_Segment("segC");
- Open_Segment("segB");
- Make_part_car2();
- Include_Segment("segC");
- Close_Segment();
- Close_Segment("?Picture");

Hoops subroutines can be used on the unix machine, DOS machine using microsoft C and DOS machine with VGA graphics card. In the work in this thesis we have used HOOPS in a unix environment on the Mathematics department's sparc stations and the Computer Science department's silicon graphics terminal (iris). The HOOPS programs were written in C and the program which generated the data were written in Fortran. The figures below are used to explain some geometry of the torus using computer graphics.

We consider these two forms of the van der Pol equation to draw the figures that follow.

$$\dot{x} = y - 0.4(x^3/3.0 - x)$$

$$\dot{y} = -x + 0.32cos(sqrt(0.84) * t). \tag{2.1.1}$$

$$\dot{x} = y$$

$$\dot{y} = (1.0 - x^2)y - x + 0.5cos(1.1t) \tag{2.1.2}$$

Fig 2.1.1 and 2.1.2 show invariant tori for (2.1.1) computed by the techniques explained in the next chapter. Fig 2.1.3 show solution trajectories computed using (2.1.1) and displayed on the spac station. For Fig 2.1.4 we use equation (2.1.2).

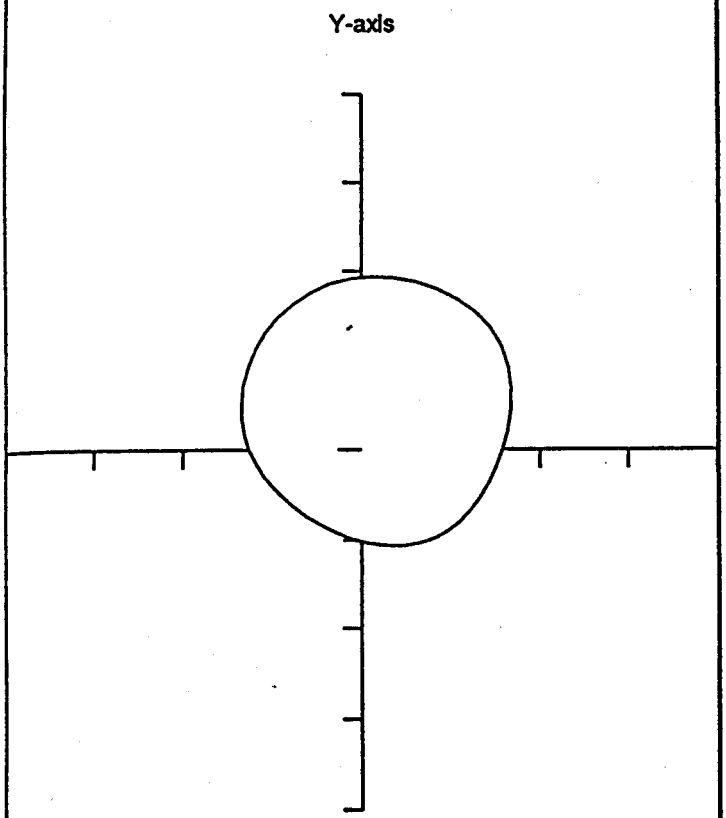

Invariant Circle

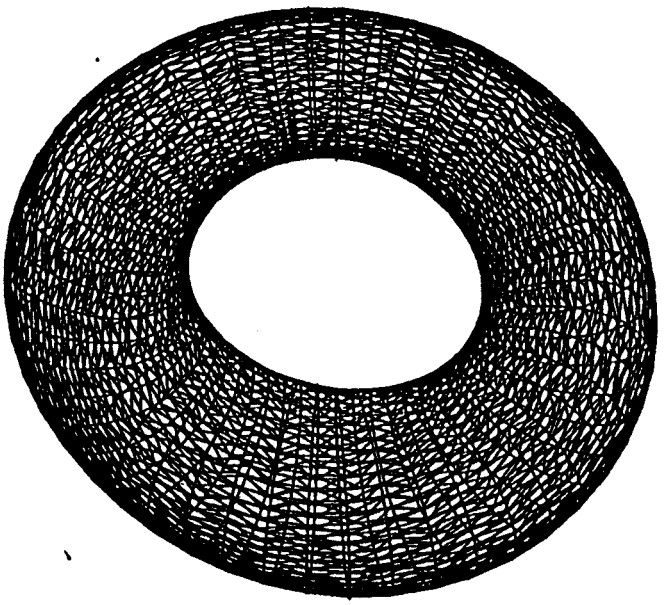

Wireframe

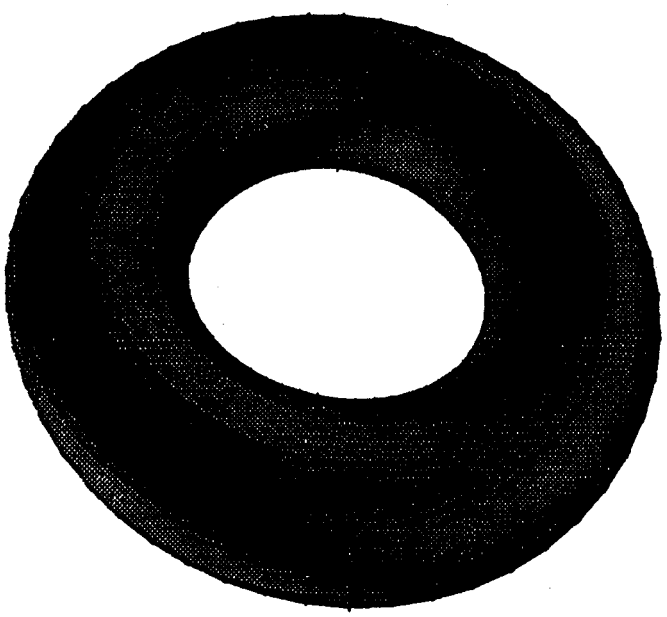

Shaded Form

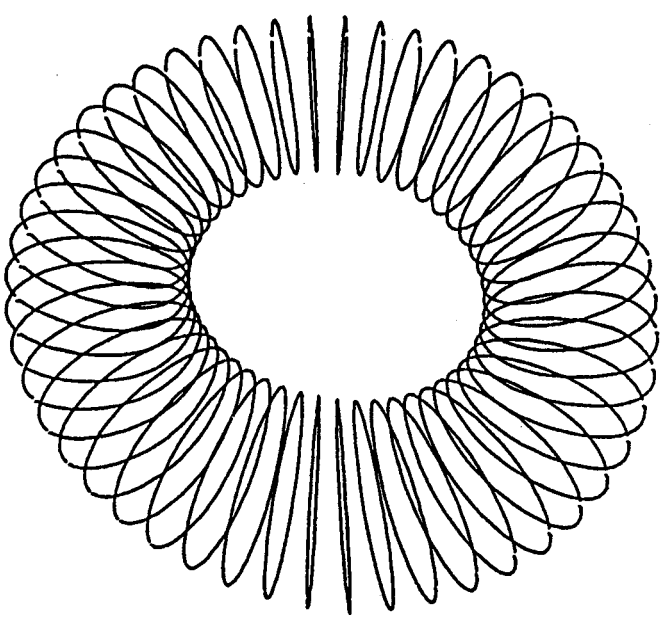

Ordinary

Fig 2.1.1

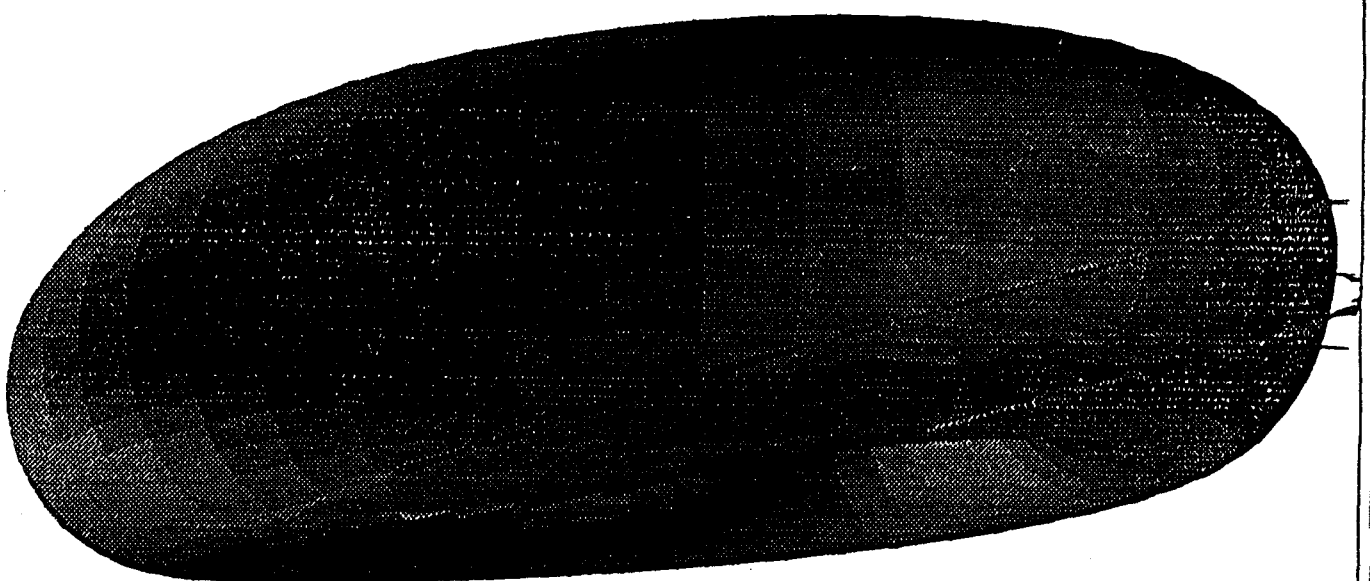

Fig 2.1.2 A trajectory on a torus

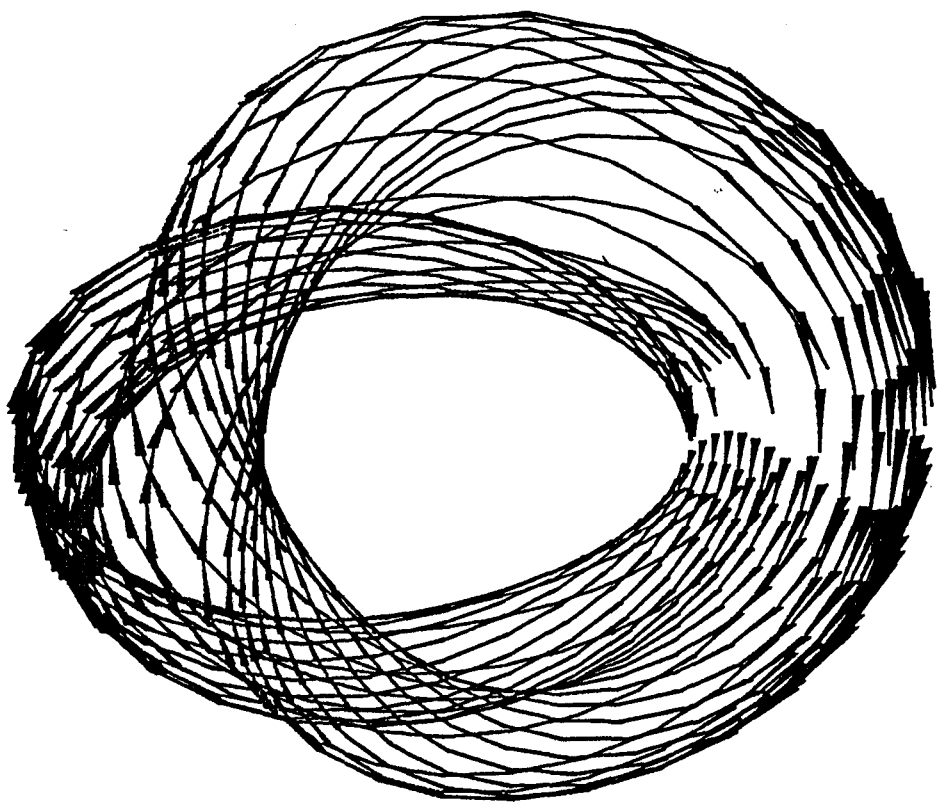

Fig 2.1.3 The flow on a torus

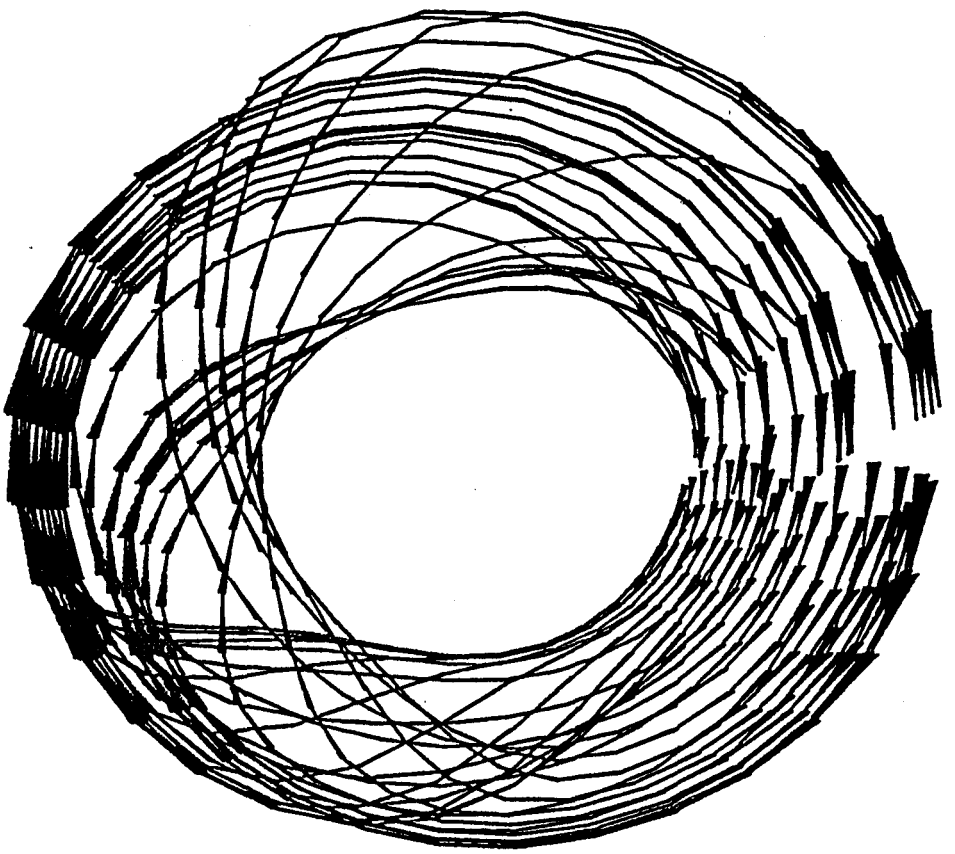

Fig 2.1.4 The flow on a torus

Chapter 3

The Poincaré map method

This chapter deals with methods that use a polygonal approximation to approximate an invariant circle. Suppose that the Jordan curve γ is an invariant curve of the map $\phi : R^d \longrightarrow R^d$, then let it be parameterised by $\tau \longrightarrow u(\tau)$. By a Jordan curve we mean a homeomorphic image of the circumference of a circle.

3.1 Coordinates

In the error analysis done by van Veldhuizen in (VVH2), he worked with two types of coordinates described below.

Assumption 3.1.1 tubular coordinates

♣ Any vector x in an annular neighborhood of $\gamma \in R^d$ can be written as

$$x = u(\tau) + z(\tau)\epsilon \tag{3.1.1}$$

where $\tau \in [0, 2\pi)$, $\epsilon \in R^{d-1}$, and $z(\tau)$ is a d x $(d-1)$ matrix with orthonormal column vectors. In addition, all columns of $z(\tau)$ are orthogonal to the vector $\frac{du}{d\tau}(\tau)$. We may even assume that the length of the vector $\frac{du}{d\tau}(\tau)$ is independent of τ♣.

In the new coordinate transformation $x \longrightarrow (\tau, \epsilon)$, the invariant curve is given by $\tau \longrightarrow (\tau, 0)$. In R^2 the matrix z reduces to the normal vector to the curve γ and the distance

$d(x;\gamma)$ of the vector x *to* γ is given by the Euclidean norm $||\epsilon||$. The invariant curve γ is attractive if there exists a constant $0 \leq \chi < 1$ such that for all x in the neighborhood of γ

$$d(\phi x;\gamma) \leq \chi d(x;\gamma). \tag{3.1.2}$$

Assumption 3.1.2 radial coordinates

♣ In an annular neighborhood of the curve γ the nonlinear coordinate transformation

$$(\theta,\rho,\nu) \longrightarrow x_c + (r(\theta)+\rho)(cos(\theta),sin(\theta),0))^T + (0,0,\psi(\theta)+\nu)^T \tag{3.1.3}$$

is a smooth invertible map, with $r(\theta) > 0$. In particular, the Jacobian matrix of the transforming map should be invertible with uniformly bounded inverse along γ♣

The curve γ can be written as

$$\gamma : \theta \in [0,2\pi) \longrightarrow \gamma(\theta) = x_c + (r(\theta)(cos(\theta),sin(\theta),\psi(\theta)))^T. \tag{3.1.4}$$

If d=2 then ψ is absent in (3.1.3) and (3.1.4) and the two equations simplify.

3.2 General format for the Poincaré methods

Let the vectors

$$x_1, x_2, x_3, \ldots, x_N$$

be the N vertices of a polygonal approximation to the invariant curve γ of the system (1.1.2). The polygon $p(\{x_i\}_{i=1}^N)$ is the set of segments $[x_1,x_2],[x_2,x_3],\ldots,[x_{N-1},x_N]$ and $[x_N,x_1]$. The polygon $p(\{x_i\}_{i=1}^N)$ is the initial approximation of the invariant curve γ at t=0 and is mapped to the polygon $p(\{Px_i\}_{i=1}^N)$. If the curve γ is attracting then the sequence of points $P^n x_i$, i=1, 2, ... gets closer to the curve γ and sometimes may converge to a point on the curve γ. We therefore find a way of redistributing the points after each mapping. The algorithm consists of 3 parts:

- 1. Compute images of the vertices of current polygonal approximation $p(\{x_i\}_{i=1}^N)$.

- 2. Project old vertices onto polygon $p(\{Px_i\}_{i=1}^N)$.
- 3. Define new polygons by taking the projection as new vertices.

Let

$$\gamma : \theta \longrightarrow x_c + (r(\theta)(cos(\theta), sin(\theta)))^T \quad \theta \in [0, 2\pi] \quad r(\theta) > 0. \tag{3.2.5}$$

Now define K as the composition of P and some projection map. Different K maps have been investigated by others as we discuss below. Let x_i be a vertex of $p(\{x_i\}_{i=1}^N)$ and the angle θ be determined such that

$$x_i = x_c + ||x_i - x_c||(cos(\theta), sin(\theta))^T$$

where x_c is the centre. Let the vertices of the polygon $p(\{Px_i\}_{i=1}^N)$ be written as

$$Px_i = x_c + \hat{r}_j(cos(\hat{\theta}), sin(\hat{\theta}))^T \tag{3.2.6}$$

and the j^{th} approximation of the polygon be given by

$$x_i^{(j)} = x_c + r_i^{(j)}(cos(\theta_i), sin(\theta_i))^T \tag{3.2.7}$$

where θ_i is independent of the number of iterations. some cases for mixed ones.

3.2.1 method 1 by van Veldhuizen

The approximation to γ is the solution to the set of equations

$$p(\{x_i\}_{i=1}^N) = p(\{Kx_i\}_{i=1}^N)$$

solved by iteration. The first nonlinear mapping K = H is described in [VVH1]. Let $x \in R^2$ be one of the points $P(x_i)$ $i = 1, ..., N$, in the neighborhood of $p(\{x_i\}_{i=1}^N)$. Assume that the minimal distance of x to x_i is at most two points. That is, there exists x_l such that

$$||x - x_l|| = min_{i=1,...N}||x - x_i|| \tag{3.2.8}$$

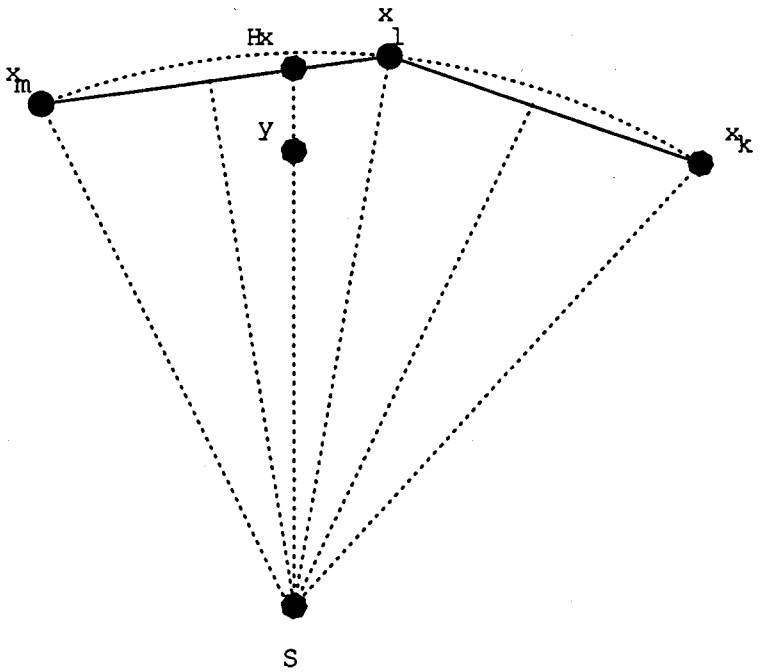

Fig. 3.2.1 : *The construction of H. The point Hx is indicated above. The projection of x on the plane formed from the successive points* x_k, x_l, x_m is y.

If there are two minimizing adjacent indices x_l and x_m for x, where $m = (l+1)mod(N+1)$, then

$$Hx = 1/2(x_l + x_m). \tag{3.2.9}$$

In the case where we have only one minimizing vector the determination of Hx is as follows: Let y be the Euclidean projection of the point x onto the 2-dimensional linear manifold determined by the vertices x_k, x_l and x_m. Let S be the centre of the circumcircle through the triangle $x_k x_l x_m$. Van Veldhuizen made the assumption that the angle between the line segments of the polygon at x_l is obtuse. Hx is defined as the intersection of the halfline $\bar{Sy}$ with the polygonal line segment $[x_k, x_l]$ *or* $[x_l, x_m]$.

Lemma 3.1.0 ♣ Let $p(\{x_i\}_{i=1}^N)$ be a given polygon and x a vector such that

- The Euclidean distance of x to the polygon $p(\{x_i\}_{i=1}^N)$ is small enough;
- The angle between any two successive line segments in the polygon is obtuse. Then

the nonlinear projection $x \longrightarrow Hx$ described above is well-defined, and H is a continuous

map.♣

Proposition 3.1.1 ♣ Assume that for all x in a tubular neighborhood of γ we have $d(Px;\gamma) \leq \kappa d(x;\gamma)$, *with* $0 \leq \kappa < 1$. If $Hx_i \in [Px_j, Px_{j+1}]$ for all i and if the x_i are close enough to γ then

$$d(Hx_i;\gamma) \leq \kappa max_{i=1,\ldots,N} d(x;\gamma) + O(||Px_j - Px_{j+1}||^2).\clubsuit \tag{3.2.10}$$

The proof is in [VVH1]. From this proposition we see that if the sequence x_i, Hx_i, $H^2x_i, \ldots$ converges for all i then the limiting polygon differs from γ by at most $O(h^2)$, where

$$h = max_{i=1,\ldots,N} ||Px_i - Px_{i+1}||.$$

3.2.2 Other methods by van Veldhuizen

Other types of possible non-linear projection are described as follows:

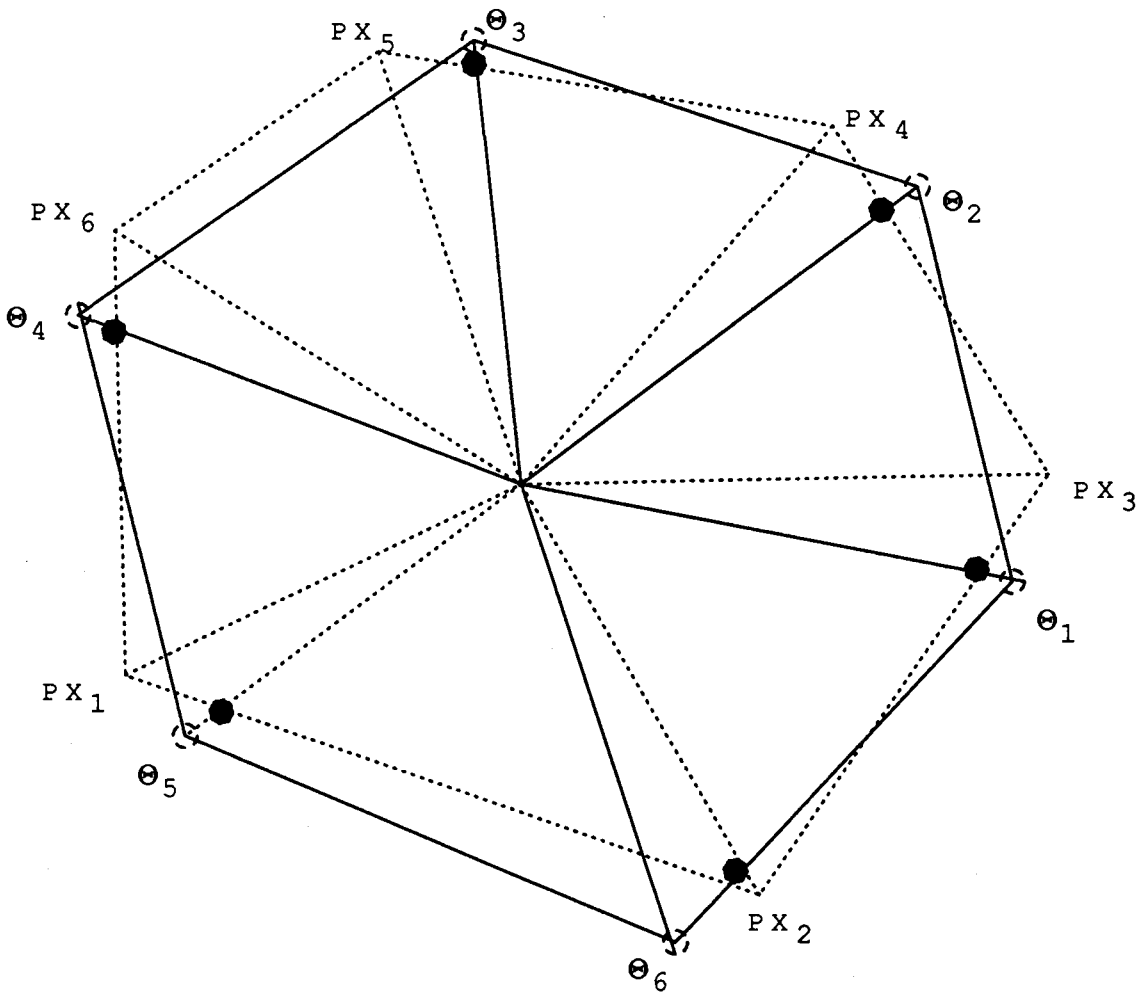

Fig 3.2.2 *Example of K_l with $N = 6$. The vertex x_i lies on the spoke θ_i indicated by the non-shaded dots. The points $K_l x_i$ are indicated by the shaded dots.*

• (i) This method is defined by the operator $K = K_l$. The method is second order, however; it is not exact if γ is a circle. The projection of a point x is defined as the intersection of the half-line in the direction of θ_i and the line segment $[Px_j, Px_{j+1}]$ and is given by

$$K_l x_i = \{x | x = x_c + r(cos(\theta_i), sin(\theta_i))^T\} \cap [Px_j, Px_{j+1}]. \qquad (3.2.11)$$

• (ii) In this and the next two cases, the projection is done using piecewise polynomial interpolation. We interpolate in the radial coordinates with abscissae on the θ -axis. First, the i^{th} vertex Kx_i of $Kp(\{x_i\}_{i=1}^N)$ is obtained using piecewise linear interpolation operator Π_1 at the point θ_i. The approximation error is given by

$$O(max_j|\hat{\theta}_j - \hat{\theta}_{j+1}|^2). \tag{3.2.12}$$

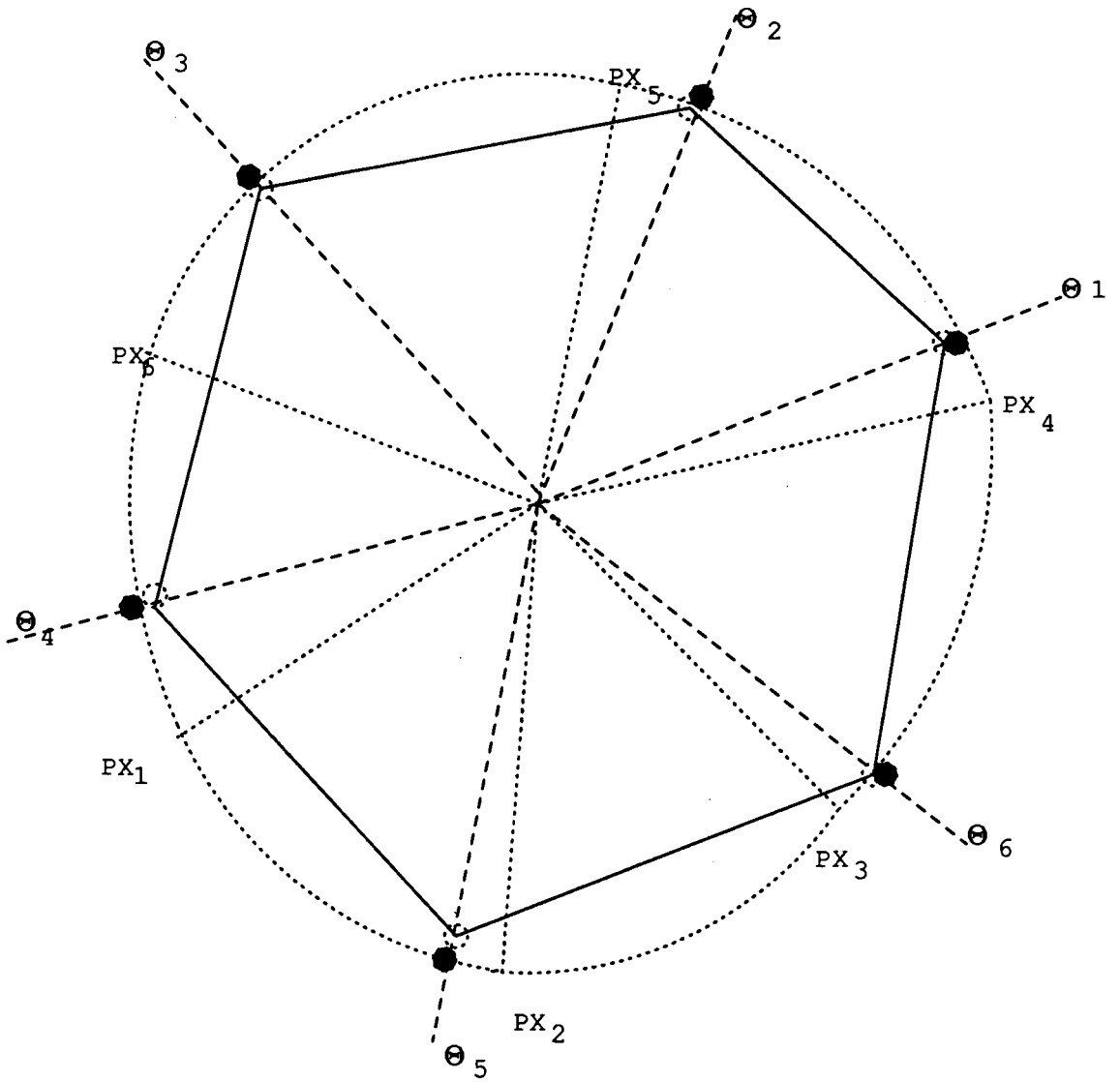

fig.3.2.5 *An example of K with* $\Pi = \Pi_1$.

•(iii) Here we use $\Pi = \Pi_3$, the piecewise cubic Lagrange interpolation polynomial such

that

$$\hat{\theta}_{j-1} < \hat{\theta}_j < \theta < \hat{\theta}_{j+1} < \hat{\theta}_{j+2}. \tag{3.2.13}$$

If we assume that

$$\mu = max_{j,k=j\pm1} \frac{\hat{\theta}_j - \hat{\theta}_{j-1}}{\hat{\theta}_k - \hat{\theta}_{k-1}} \tag{3.2.14}$$

then it is shown in [VVH2] that

$$\frac{5}{2}\mu \geq |\Pi_3| \geq 1 + \frac{\mu^2}{2(\mu+1)}. \tag{3.2.15}$$

The error is given by

$$O(max|\hat{\theta}_j - \hat{\theta}_{j+1}|^4). \tag{3.2.16}$$

•(iv) The last projection operator $\Pi = \Pi_s$ is the cubic spline interpolation polynomial. Let

$$\nu = max_{i,j} \frac{\hat{\theta}_{j+1} - \hat{\theta}_j}{\hat{\theta}_{i+1} - \hat{\theta}_i}. \tag{3.2.17}$$

then the norm of the spline interpolation operator is bounded by

$$|\Pi_s| \leq 1 + s\nu^2. \tag{3.2.18}$$

We consider Π_1, Π_3, Π_s as projection operators in the Banach space of continuous functions on $[0, 2\pi)$ equipped with the usual supremum norm of functions.

K has the following properties:

Lemma 3.2.1 ♣ There exists a constant $C_d \geq 1$ such that for all x in an annular neighborhood of γ, we have

$$d(Kx;\gamma) \leq d_{rad}(x;\gamma) \leq C_d d(x;\gamma). \tag{3.2.19}$$

The constant C_d depends on the position of x_c in the interior of the projection of γ onto R and the size of the annular neighborhood. ♣

The distance $d_{rad}(x;\gamma)$ is the radial coordinate distance from $x = (\theta, \rho, \nu)$ to γ and is given by the Euclidean length of the vector (ρ, ν).

Lemma 3.2.2 ♣ For $P(\{x_i\}_{i=1}^N)$ close enough to γ

$$d_{rad}(Kx_i, \gamma) \leq \tau C_d |\Pi|_{m_{i=1\ldots N}} max \;\; d(x_i, \gamma) + |\pi_\gamma - \gamma|.\clubsuit \tag{3.2.20}$$

Theorem 3.2.3 ♣ If $\tau C_d|\Pi| < 1$ and if the interpolation error is sufficiently small, then the equation $p(\{x_i\}_{i=1}^N) = p(\{Kx_i\}_{i=1}^N)$ has at least one solution in the closure of an annular neighborhood of γ. The radial distance from points in this neighborhood to γ is bounded by

$$\delta = \frac{|\Pi_\gamma - \gamma|}{1 - \tau C_d |\Pi|_m}.\clubsuit \tag{3.2.21}$$

Theorem 3.2.4 ♣ In addition to the assumptions of Theorem (3.2.3), let Π be the piecewise linear interpolation operator (on the abscissae $\hat{\theta}_j$), and let the interpolation error be sufficiently small. Then the equation has a unique solution $p(\{\bar{x}_i\}_{i=1}^N)$ and the sequence $p(\{x_i\}_{i=1}^N)$, $p(\{Kx_i\}_{i=1}^N)$,$p(\{K^2x_i\}_{i=1}^N)$,... converges to it with a convergence factor $\leq \chi'$, *where* $C_d\,\chi < \chi' < 1$. ♣

Assumption 3.2.5 ♣ In a sufficiently small annular neighborhood of γ we have

$$||Px - Py|| \leq \bar{\chi}||x - y|| \tag{3.2.22}$$

for x, y vectors with the same θ - coordinate (on the same half-line centered in x_c).♣

Theorem 3.2.6 ♣ Under the above assumption, in particular assumption 3.2.5, let $P(\{x_i\}_{i=1}^N)$ belong to a sufficiently small annular neighborhood of γ. Let Π be the operator defined by piecewise linear interpolation. Let $\bar{\chi}|\Pi|_m < 1$. Then the sequence $P(\{x_i\}_{i=1}^N)$, $P(\{Kx_i\}_{i=1}^N)$, $P(\{K^2x_i\}_{i=1}^N)$,... converges to a unique polygon $P(\{\bar{x}_{i=1}^N\})$. The discretization error satisfies the estimate

$$max_{i=1,\ldots,N} d(\bar{x}_i; \gamma) \leq \frac{|\Pi\gamma - \gamma|}{[1 - \bar{\chi}]|\Pi|_m}.\clubsuit \tag{3.2.23}$$

3.3 Newton's Method (Kevrekidis)

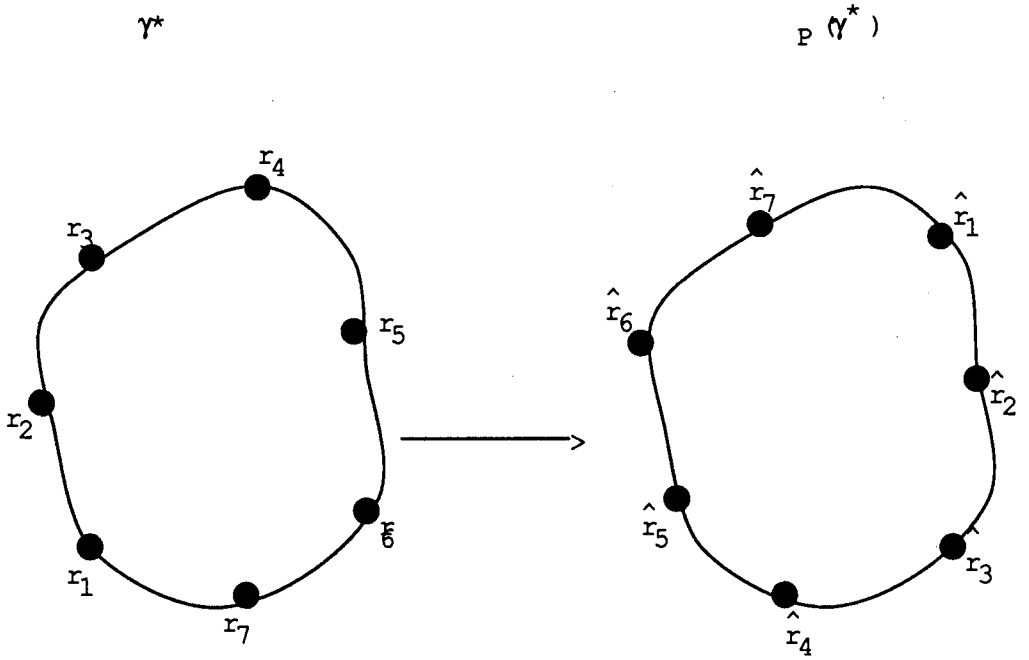

fig.3.3.1 Due to the rotational effect of P, P(x) $\neq$ x for all x $\in \gamma$.

The Newton-Raphson method can be used to solve the system

$$p(\{x_i\}_{i=1}^N) = p(\{Kx_i\}_{i=1}^N).$$

Define $r_k := r(\theta_k)$ for k=1, ...,N where $\theta_k = 2\pi(k-1)/N$. Let $\hat{r} : S^1 \longrightarrow R^+$ be the radius function obtained by interpolation of $\hat{r}_k$ and $\hat{\theta}_k$, that is

$$\hat{r}_k = P \; o \; r(\theta_k) = \hat{r}(\hat{\theta}_k), \tag{3.3.24}$$

and

$$H(r_1, r_2, ...r_N) := \begin{bmatrix} r_1 \\ r_2 \\ \vdots \\ r_N \end{bmatrix} - \begin{bmatrix} \hat{r}(\theta_1) \\ \hat{r}(\theta_2) \\ \vdots \\ \hat{r}(\theta_N) \end{bmatrix}.$$

The function $\hat{r}$ is based on interpolation of $\hat{r}_k$ and is denoted by $\hat{r}(\theta : r_1, r_2, ..., r_N)$ and

$$h_{ik} = \delta_{jk} - \frac{\partial \hat{r}(\theta_j)}{\partial r_k} \tag{3.3.25}$$

where $\frac{\partial \hat{r}(\theta_j)}{\partial \hat{r}_k}$ is dependent on the interpolation used. For linear interpolation

$$\hat{r}(\theta_j) = (1-\alpha)\hat{r}_k + \alpha \hat{r}_{k+1} \tag{3.3.26}$$

where $\hat{\theta}_k < \theta_j < \hat{\theta}_{k+1}$ and

$$\alpha := \frac{(\theta_j - \hat{\theta}_k)}{(\hat{\theta}_{k+1} - \hat{\theta}_k)}. \tag{3.3.27}$$

DH is sparse and has a non-zero band which is of a special interest. The band lies away from the diagonal of the matrix due to rotational effect of P. If, however, it does cross the diagonal, at row j on convergence, say, then there is a fixed point on the invariant curve.

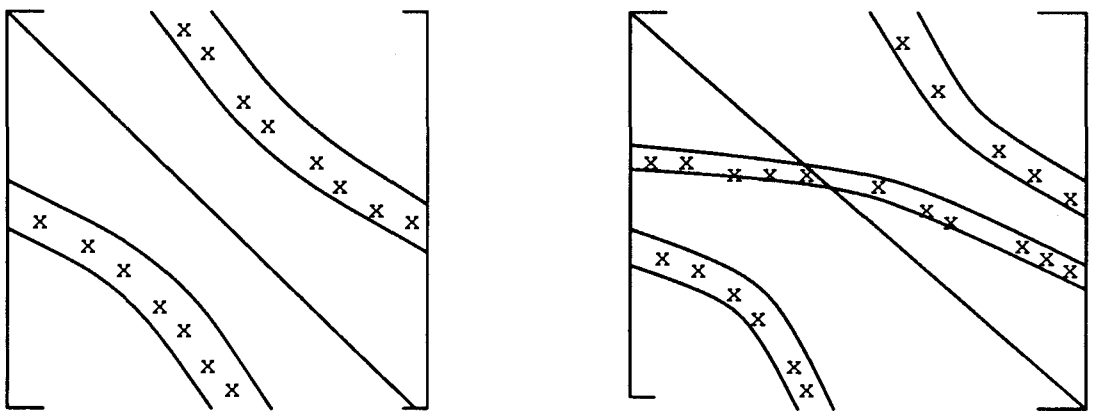

(a) (b)

fig.3.3.2 (a) The structure of the Jacobian. (b) The Jacobian after convergence when there is a fixed point on the invariant curve.

3.4 The Hadamard graph transform approach

This is a variation of the Poincaré map methods and was proposed by Dieci, Lorenz and Russell [DLR]. In this case the non-linear map involves solving a boundary value problem and the set of equations

$$p(\{x_i\}_{i=1}^N) = p(\{Kx_i\}_{i=1}^N)$$

is also solved by iteration. This algorithm works for attracting or repelling invariant curves as in the general Poincaré map methods and can be modified to work for the mixed ones.

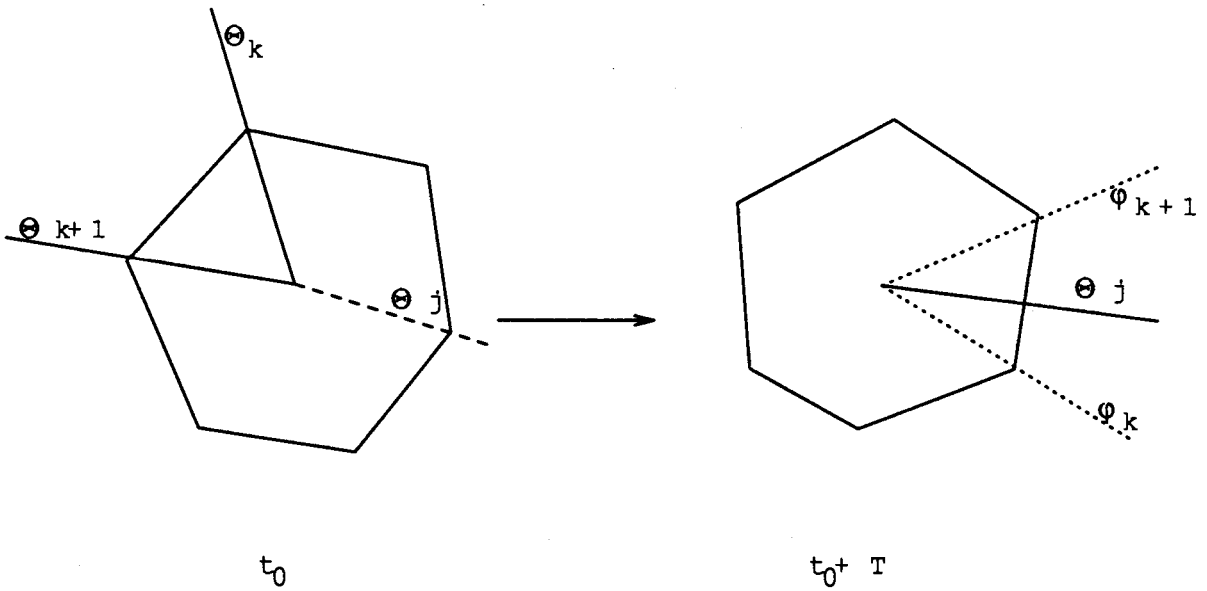

Fig 3.3.4 *The Poincare map of the points x_k, x_{k+1} with angular parts θ_k, θ_{k+1} respectively.*

Let the image of x_k, x_{k+1} with angular parts θ_k, θ_{k+1} be Px_k, Px_{k+1} with angular part $\varphi_k, and\ \varphi_{k+1}$ respectively. We then parameterised the segment $[x_k,\ x_{k+1}]$ in θ and interpolate r along this segment . Using bisection or the secant method we can find the point x which integrates to y with angular part θ_j. (See fig 3.3.5)

The algorithm is as follows:

- Choose

  (a) an initial polygon $p(x_{i}{}_{i=1}^{N})$

  (b) δ tolerance

  (c) M_{max} maximum number of iterations

- Compute $p(Px_{i}{}_{i=1}^{N})$ by integrating the differential equation (1.1.2) using the standard integrators like RKF45 and ODE.

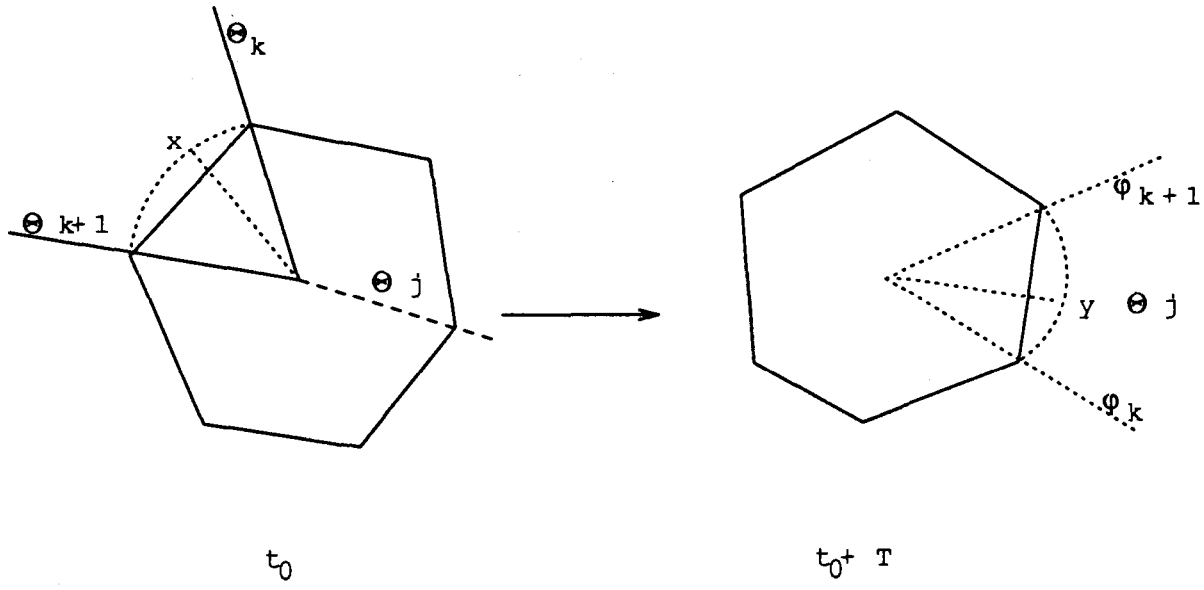

Fig 3.3.5 *The point x maps onto y.*

- Find the two points x_k, x_{k+1} with angular parts θ_k and θ_{k+1} respectively which integrate to Px_k, Px_{k+1} with angular parts φ_k *and* φ_{k+1} respectively such that $(\varphi_k,\ \varphi_{k+1})$ contains θ_j, the angular part of the point to be updated.

- For each θ_j find a point x along the half-line θ_k *and* θ_{k+1} which integrates to y with angular part θ_j. The point x along θ_k and θ_{k+1} has the radial part interpolated using linear interpolation.

- Let $Gx = y$. If $M > M_{max}$ or $max|Gx_i - x_i| < tol$ update the polygon and exit; else goto step 2.

Chapter 4

The pde approach

4.1 The pde approach

The method is introduced by Dieci, Lorenz and Russell in their paper[DLRR]. In this approach they compute an invariant manifold for a finite dimensional dynamical system by assuming that the manifold can be parameterised over a torus in terms of subset variables. The approach then involves solving a system of partial differential equations subject to periodic boundary conditions.

Consider the autonomous system

$$\frac{d\vec{w}}{dt} = \vec{f}(\vec{w}), \qquad \vec{w} \in W \subset R^n, \tag{4.1.1}$$

$\vec{f} : R^n \longrightarrow R^n$ is smooth. Assume there is a smooth manifold $M \subset W$ invariant under the flow (4.1.1). If S^t is the solution operator of (4.1.1) and

$$\vec{w}(0) = \vec{w}_0 \in M, \tag{4.1.2}$$

then the solution is

$$\vec{w}(t) = S^t \vec{w}_0 \in M. \qquad -\infty < t < \infty. \tag{4.1.3}$$

We are interested in the special case where (4.1.1) may be written in the form

$$\frac{d\vec{u}}{dt} = \vec{f}(\vec{u}, \vec{v})$$

$$\frac{d\vec{v}}{dt} = \vec{g}(\vec{u},\vec{v}), \qquad \vec{w} = (\vec{u},\vec{v}) \in U \times V = W. \tag{4.1.4}$$

There exists a manifold

$$M = \{(\vec{u}, \Phi(\vec{u})) : \vec{u} \in U\}$$

which can be parameterised over U. Let $\vec{v} = \Phi(\vec{u})$, then

$$\Phi'(\vec{u}) f(\vec{u}, \Phi(\vec{u})) = g(\vec{u}, \Phi(\vec{u})), \qquad \vec{u} \in U. \tag{4.1.5}$$

Letting dim U = p and dim V = q then (4.1.5) is a system of partial differential equations for

$$\Phi_1(u_1, u_2, ...u_p), ..., \Phi_q(u_1, u_2, ...u_p). \tag{4.1.6}$$

To solve (4.1.5), we discretize on a fixed grid by the leap frog scheme and then solve with Newton's method. *This approach can give convergence independent of the attractivity of M.* The stability of the discretization and its independence of attractivity properties was proved for simple models in [DLRR].

For the case where U is a 2-torus and V is the real line, (4.1.5) is linear and is related to the Poincaré map for the original equation. By parameterizing (4.1.4) and solving (4.1.5) approximately linearised by the method of characteristics we retrieve the method of van Veldhuizen. In the case where U is a p-torus denoted by

$$T^p = \{\vec{\theta} = (\theta_1, \theta_2, ..., \theta_p) : \theta_j \in R(mod 2\pi)\}, \tag{4.1.7}$$

equation (4.1.4) becomes

$$\frac{d\vec{\theta}}{dt} = \vec{f}(\vec{\theta}, \vec{r})$$

$$\frac{d\vec{r}}{dt} = \vec{g}(\vec{\theta}, \vec{r}) \text{ where } (\vec{\theta}, \vec{r} \in T^p \times R^q). \tag{4.1.8}$$

The manifold M given by

$$M := \{(\vec{\theta}, \vec{r}(\vec{\theta})) : \vec{\theta} \in T^p\} \subset T^p \times R^q \tag{4.1.9}$$

can be determined by solving the pde

$$\sum_{j=1}^{p} = f_j(\vec{\theta}, \vec{r}(\vec{\theta})) \frac{\partial \vec{r_i}}{\partial \theta_j}(\vec{\theta}) = \vec{g}(\vec{\theta}, \vec{r}(\vec{\theta})), \quad \theta \in T^p, \quad i = 1, ..., q \tag{4.1.10}$$

subject to the periodic boundary conditions

$$r_i(\theta_1,...\theta_{k-1},0,\theta_{k+1},...\theta_p) = r_i(\theta_1,...\theta_{k-1},2\pi,\theta_{k+1},...\theta_p) \tag{4.1.11}$$

$$i = 1,...,q, \quad k = 1,...,p$$

for the unknown (smooth) function $\vec{r}: T^p \longrightarrow R^q$. For the case p=2 and q=1 we obtain

$$f_1(\vec{\theta},r)r_{\theta_1} + f_2(\vec{\theta},r)r_{\theta_2} = g(\vec{\theta},r), \quad \vec{\theta} \in [0,2\pi]\times[0,2\pi]$$

$$r(0,\theta_2) = r(2\pi,\theta_2), r(\theta_1,0) = r(\theta_1,2\pi). \tag{4.1.12}$$

We linearize (4.1.12) and use Newton's iteration starting with $r^0 = r^0(\vec{\theta})$ which satisfies (4.1.12). Then r^1 is also a solution of (4.1.12) and

$$b_1(\vec{\theta})r^1_{\theta_1} + b_2(\vec{\theta})r^1_{\theta_2} + c(\vec{\theta})r^1 = q(\vec{\theta}) \tag{4.1.13}$$

where

$$b_1(\vec{\theta}) := f_1(\vec{\theta},r^0), \quad b_2(\vec{\theta}) := f_2(\vec{\theta},r^0),$$

$$c(\vec{\theta}) := -g_r(\vec{\theta},r^0) + f_{1r}(\vec{\theta},r^0)r^0_{\theta_1} + f_{2r}(\vec{\theta},r^0)r^0_{\theta_2}, \tag{4.1.14}$$

$$q(\vec{\theta}) := g(\vec{\theta},r^0) - [g_r(\vec{\theta},r^0) - f_{1r}(\vec{\theta},r^0)r^0_{\theta_1} + f_{2r}(\vec{\theta},r^0)r^0_{\theta_2}]r^0.$$

In the case p=2 q=2 we obtain

$$f_1(\vec{\theta},\vec{r}(\vec{\theta}))\begin{bmatrix} \frac{\partial r_1}{\partial\theta_1} \\ \frac{\partial r_2}{\partial\theta_1} \end{bmatrix} + f_2(\vec{\theta},\vec{r}(\vec{\theta}))\begin{bmatrix} \frac{\partial r_1}{\partial\theta_2} \\ \frac{\partial r_2}{\partial\theta_2} \end{bmatrix} = \begin{bmatrix} g_1(\vec{\theta},\vec{r}(\vec{\theta})) \\ g_2(\vec{\theta},\vec{r}(\vec{\theta})) \end{bmatrix} \tag{4.1.15}$$

$$r_i(0,\theta_2) = r_i(2\pi,\theta_2), r_i(\theta_1,0) = r_i(\theta_1,2\pi) \quad i = 1,2.$$

Chapter 5

Comparison of the three Methods

The programming in this section was done on the Mathematics department Sparc stations and the plots were done using the software Gnuplot. I obtained the pde program from Dieci et al. and the Hadamard graph transform program was written in conjunction with Russell and McCorquadale (currently a student at the Mathematics Dept, Univ of Berkeley, California).

The methods considered were applied to

(1) the van der Pol oscillator.

(2) the Coupled oscillator.

(3) the Delayed logistic map.

5.1 The van der Pol Oscillator

The van der Pol oscillator equation arose as a model in electric circuit theory (1927). Van der Pol used it to model an electric circuit with a triode valve. The resistive properties of the valve change with the current such that low current negative resistance becomes positive as the current increases. The single degree of freedom limit cycle oscillators are similar to the unforced van der Pol system which occur in

- models of wind-induced oscillations of buildings due to vortex shedding. (Novak, Davenport [1970] etc.).
- in stability studies of both tracked and rubber tired vehicles.
- certain models of chemical reactions.

The equation is given by

$$\ddot{x} + \alpha(x^2 - 1)\dot{x} + x = \beta cos(\omega t). \tag{5.1.1}$$

Under the transformations

$$p(x) = x^3/x - x$$

$$y = \dot{x} + \alpha p(x), \tag{5.1.2}$$

we obtain

$$\dot{x} = y - \alpha p(x)$$

$$\dot{y} = -x + \beta cos(\omega t). \tag{5.1.3}$$

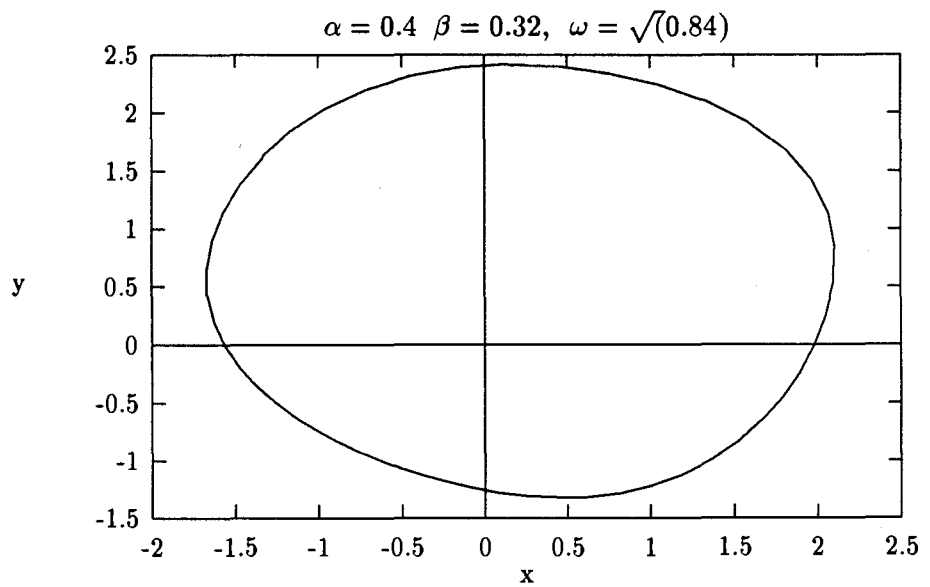

fig 5.1.1 *The invariant circle of the van der Pol oscillator with parameters as shown above.*

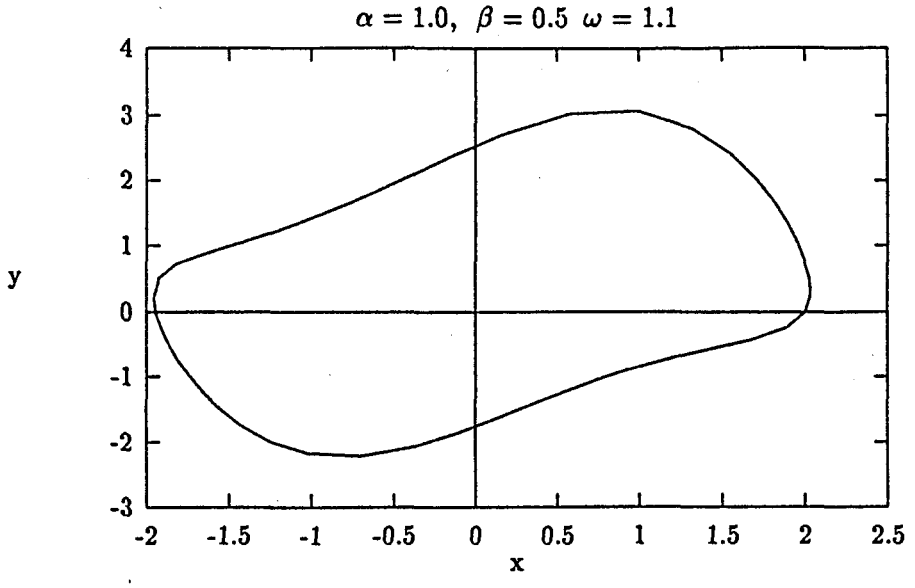

fig 5.1.2 *The invariant circle of the van der Pol oscillator with the transformation* $\dot{x} = y,\ \dot{y} = \alpha(1-x^2)y - x + \beta cos(\omega t)$.

We now apply the method of van Veldhuizen, the pde method and the Hgt approach to a deforming torus for the van der Pol equation (5.1.2). Fig(5.1.3) is from (VVH1).

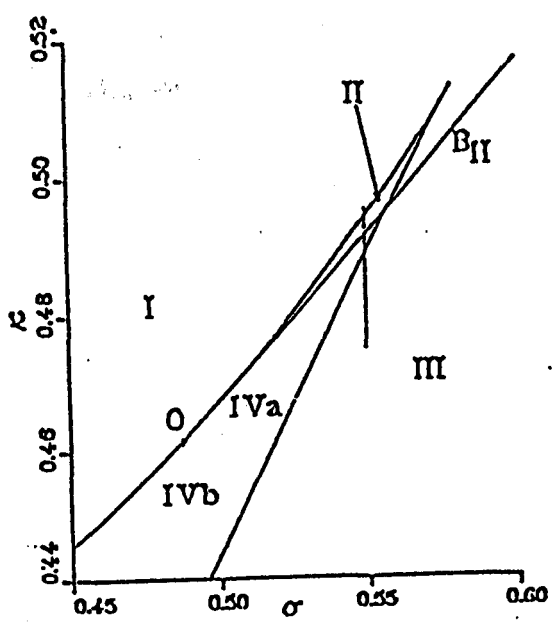

fig 5.1.3 *A portion of the* σ, κ *plane from Guckenheimer and Holmes. The region I-IV are the same as in the text. The dotted line* $\sigma = 0.55$ *is our line of interest. The region III*

has an invariant torus.

The invariant curves for the κ values (0) 0.4925 (1) 0.49, (2) 0.48875, (3) 0.48750, (4) 0.48625, (5) 0.485, (6) 0.48375 (7) 0.4825 (8) 0.48, (9) 0.475. with $\sigma = 0.55$ and $\alpha = 0.4$ were used as our test problems. When we tried the pde code for this problem, we had convergence for the κ value 0.475(9) only. This may be due to the poor initial guess for r.

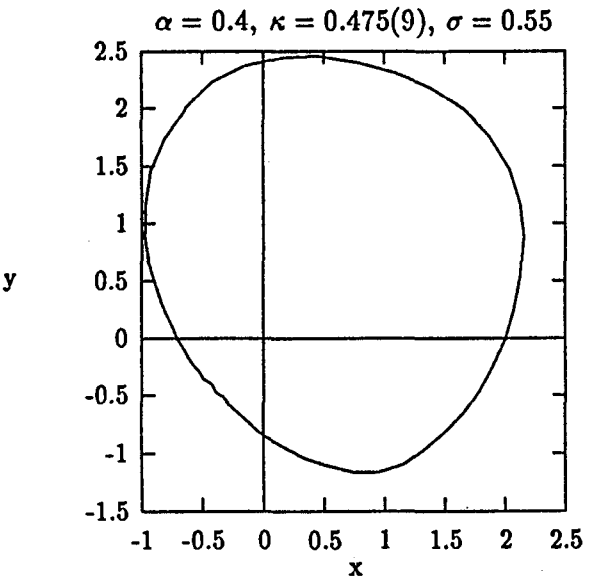

fig 5.1.4 *The invariant circle of the van der Pol oscillator using the pde approach.*

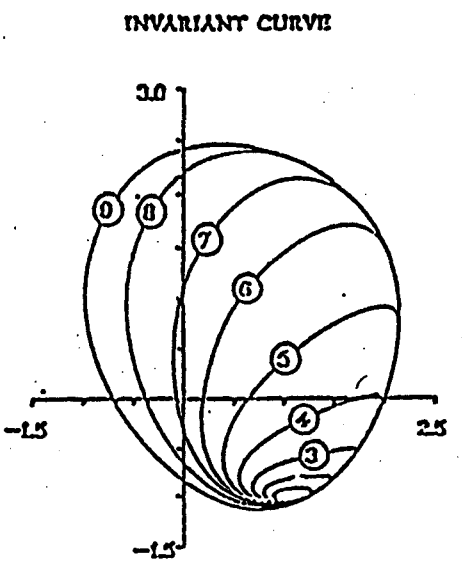

fig 5.1.5 *The invariant curves computed by van Veldhuizen [VVH1].*

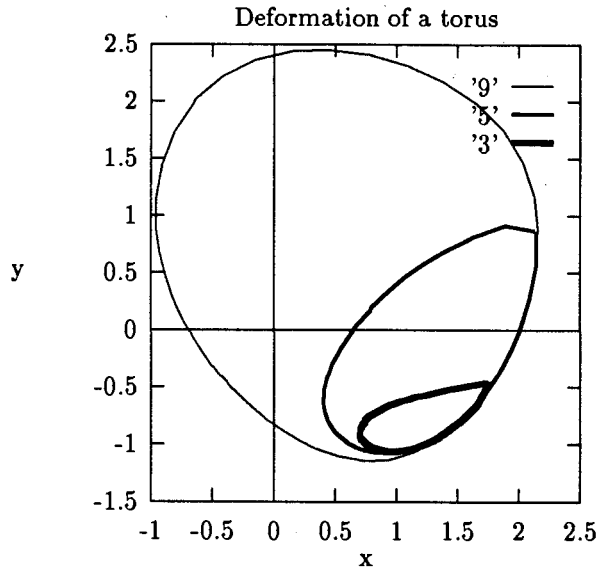

fig 5.1.6 *The invariant circles using Hadamard Graph Transform.*

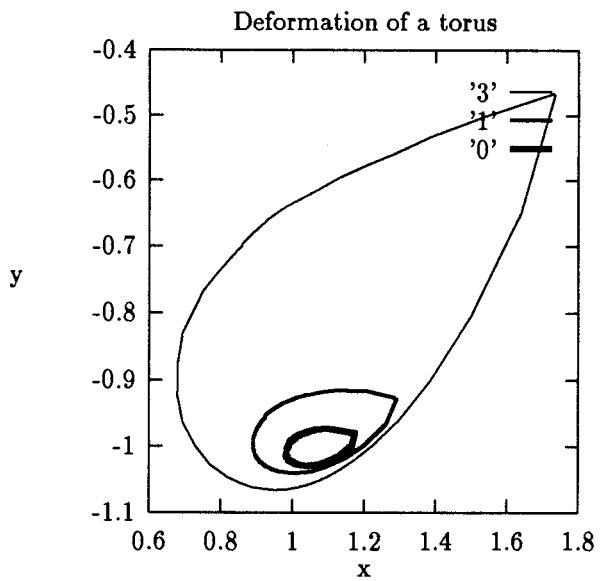

fig 5.1.7 *The invariant circles using Hadamard Graph Transform.*

With the Hadamard Graph Transform we were able to compute the invariant circle for $\kappa = 0.4925$ which was a step further than the results of [VVH1] in the direction of the deforming torus. The Hadamard graph transform used less computer time compared to the other two.

κ	Van Veldhuizen	Hgt approach	pde approach
0.475	Not done	Converged	Did not converge
0.48	Converged	Converged	Did not converge
0.4825	Converged	Converged	Did not converge
0.48375	Converged	Converged	Did not converge
0.485	Converged	Converged	Did not converge
0.48625	Converged	Converged	Did not converge
0.48750	Converged	Converged	Did not converge
0.48875	Converged	Converged	Did not converge
0.49	Converged	Converged	Did not converge
0.4925	Converged	Converged	Converged

Table 1. *Comparison of the three methods using the van der Pol oscillator.*

5.2 Coupled Oscillators

The next problem we consider is that involving the coupled oscillator equation. It is used to model a wide variety of systems in the biological and physical sciences. They arise for example in the study of

- oscillating organic reactions in models of neutral network and intestimal waves.
- circadian rhythms and cell-cycle phenomena in pattern formation.

Here we consider the dynamics of 2-coupled planar oscillators which give rise to a system of ordinary differential equations in R^4. Each oscillator has a unique periodic solution that is attracting and the coupled product system has a unique invariant torus that is attracting. The torus persists for weak coupling and contains 2-periodic solutions when the coupling is linear and conservative. However the torus disappears for strong coupling. Thus we want to understand the behaviour during the deformation stage.

The equation is given by

$$\begin{aligned}
\dot{x_1} &= \alpha_1 x_1 + \beta_1 y_1 - (x_1^2 + y_1^2)x_1 - \delta(x_1 + y_1 - x_2 - y_2) \\
\dot{y_1} &= \alpha_1 y_1 - \beta_1 x_1 - (x_1^2 + y_1^2)y_1 - \delta(x_1 + y_1 - x_2 - y_2) \\
\dot{x_2} &= \alpha_2 x_2 + \beta_2 y_2 - (x_2^2 + y_2^2)x_2 + \delta(x_1 + y_1 - x_2 - y_2) \\
\dot{y_2} &= \alpha_2 y_2 - \beta_2 x_2 - (x_2^2 + y_2^2)y_2 + \delta(x_1 + y_1 - x_2 - y_2).
\end{aligned} \tag{5.2.4}$$

The symbol δ is the coupling parameter. When $\delta = 0$ the two oscillators have distinct attracting limit cycles given by $x_i^2 + y_i^2 = \alpha_i$. Making the transformation $x_i = r_i cos\theta_i$ *and* $y_i = -r_i sin\theta_i$ $i = (1,2)$ and using -θ we obtain

$$\begin{aligned}
\dot{\theta_1} &= \beta_1 + \delta(cos2\theta_1 - r_2/r_1[sin(\theta_1 - \theta_2) + cos(\theta_1 + \theta_2)] \\
\dot{\theta_2} &= \beta_2 + \delta(cos2\theta_2 - r_2/r_1[sin(\theta_1 + \theta_2) + cos(\theta_1 - \theta_2)] \\
\dot{r_1} &= r_1(\alpha_1 - r_1^2) - \delta\{r_1(1 - sin2\theta_1) + r_2[sin(\theta_1 + \theta_2) - cos(\theta_1 - \theta_2)]\}
\end{aligned} \tag{5.2.5}$$

$$\dot{r_2} = r_2(\alpha_2 - r_2^2) - \delta\{r_2(1 - sin2\theta_2) - r_1[sin(\theta_1 + \theta_2) - cos(\theta_1 - \theta_2)]\}.$$

The Hadamard graph transform approach was used to compute the invariant circles for the parameter values $\alpha_1 = \alpha_2 = 1$, $\beta_1 = \beta_2 = 0.55$, and $\delta = 0.0,\ 0.05,\ 0.10,\ 0.15$.

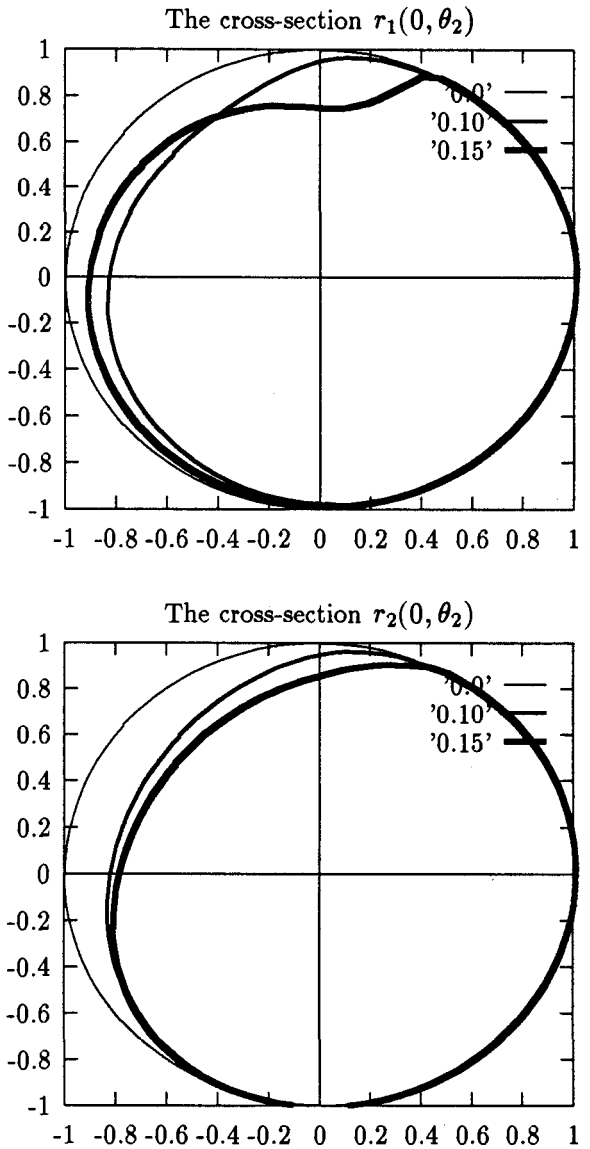

Fig 5.2.1 *The invariant curves computed using the Hadamard Graph Transform approach for the δ values 0.0, 0.05, 0.10, 0.15.*

The pde approach [DLRR] was used to compute the invariant circles at the parameter values $\delta = 0.23 - 0.22527$ and using a second transformation

$$r_i = \sqrt{\alpha_i} + \delta z_i.$$

The results of the Hadamard graph transform approach begin to differ from the pde approach at values of δ higher than 0.1 The Hadamard graph transform used far less computer time compared to the pde approach.

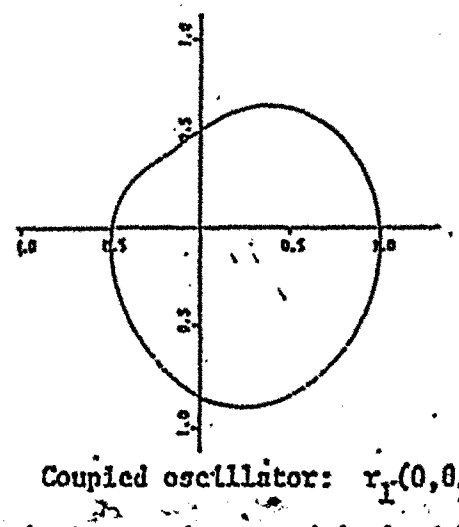

Fig 5.2.2 *The invariant curves computed using the pde approach for* $\delta = 0.23$.

δ	Hgt approach	pde approach
0.00	Converged	Not done
0.10	Converged	Not done
0.15	Converged	Not done
2.23	Not done	Converged

Table 2. Comparison using two coupled oscillator equation.

5.3 Delayed Logistic Map

This model is used in population dynamics and is given by

$$N_{n+1} = aN_n(1.0 - N_{n-1}) \tag{5.3.6}$$

where N_n is the population in the n^{th} generation. If we set

$$x_n = N_{n-1}, \qquad y_n = N_n,$$

we obtain

$$F_a(x_n, y_n) = (x_{n+1}, y_{n+1}) = (y_n, ay_n(1.0 - x_n)). \tag{5.3.7}$$

The fixed points (x^*, y^*) of the map F_a is given by

$$F_a(x^*, y^*) = (x^*, y^*). \tag{5.3.8}$$

Solving (5.3.8) we get $(x^*, y^*) = (0,0)$ or $\frac{a-1}{a}(1,1)$. The fixed point $\frac{a-1}{a}(1,1)$ is stable for $1 < a \leq 2$. It losses stability and spawns an invariant circle via a Hopf bifurcation as the parameter a passes through 2.

The program using the Hadamard graph transform approach was applied to the delayed logistic map

$$(x, y) \longrightarrow \Phi(x, y) = (y, ay(1 - x)) \tag{5.3.9}$$

which for values of $a > 2.17$ has invariant curves that are topologically circles.

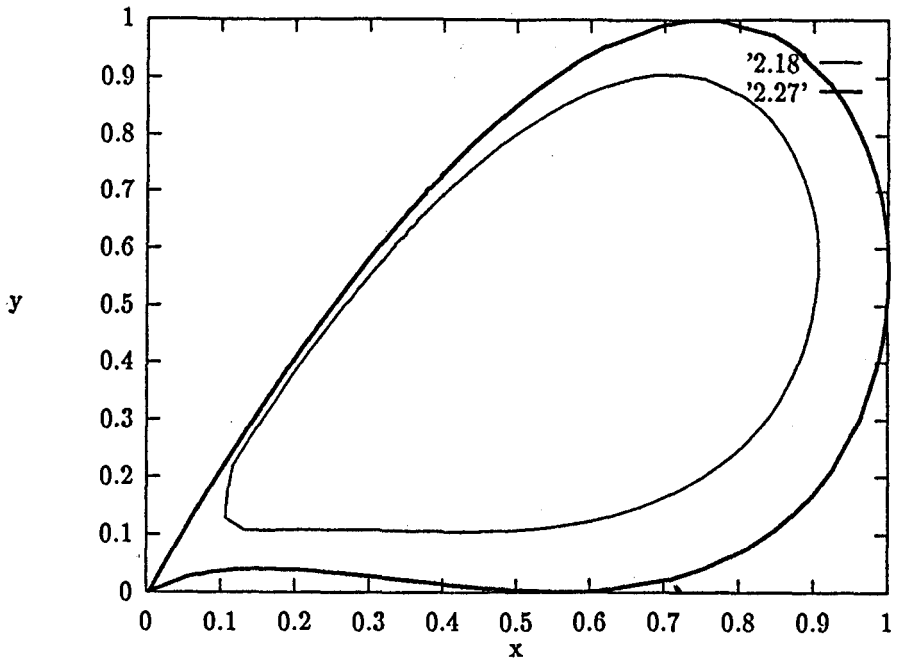

Fig 5.3.1 *The invariant curves for the delayed logistic map for the a values 2.18 and 2.27.*

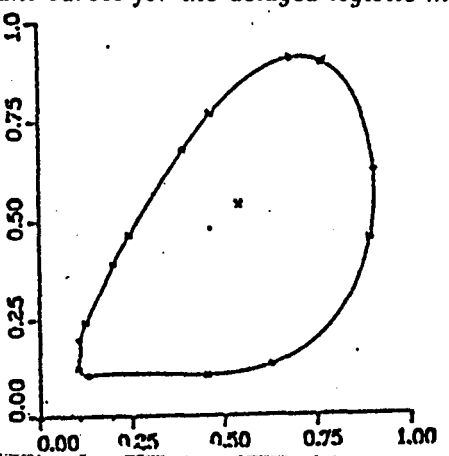

Fig 5.3.2 *The invariant curve for the delayed logistic map for a = 2.18 by van Veldhuizen.*

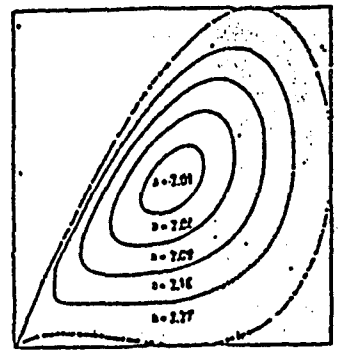

Fig 5.3.3 *The invariant curves for the delayed logistic map using direct iteration of the map by Aronson et al. [ACHM]. Each circle needed 1000-2500 iterates of the map.*

With our program we were able to compute the circle for $a = 2.27$. Van Veldhuizen was able to get the invariant curves to only $a = 2.18$. For these two methods we required a good initial guess for the first iterate. In the case of storage Van Veldhuizen used 1400 points to compute the invariant circle at $a = 2.18$ while our method used 50 points to get almost the same curve.

a	Van Veldhuizen	Hgt approach
2.01	Converged	Converged
2.04	Converged	Converged
2.18	Converged	Converged
2.27	Not done	Converged

Table 3. Comparison of the delayed logistic map.

Chapter 6

Other methods of computing a torus

In this section we mention other possible numerical methods. While these have not proven to be competitive with those previously mentioned (eg. [VVH1]), it may be that suitable modifications would lead to significant improvement in their performance.

6.1 Chan's Method

He proposed two methods, one of which uses the concept of rotation numbers and approximates the invariant circle by a truncated Fourier Series and was modified using a cubic B-splines representation. The second is similar to the first but with some modifications.

In the Fourier series approach he represents the invariant circle by a truncated Fourier series

$$u(t) = a_0 + \sum_{k=1}^{m}(a_k sin(kt) + b_k cos(kt)) \tag{6.1.1}$$

$$a_0, a_k, b_k \in R^2, \qquad k = 1, 2, ..., m.$$

Let ψ be a two-dimensional diffeomorphism $\psi : R^2 \longrightarrow R^2$ such that $\psi(u(t))$ is a rotation

on the circle $u(t)$) and let τ be the rotation number of the circle $u(t)$ so that

$$\psi_\lambda(u(t)) = u(t+\tau). \tag{6.1.2}$$

Using $2m+1$ equally spaced time step collocation points with $t_i = idt$, i=1,...,2m+1 and $dt = 2\pi/(2m+1)$, we obtain the discrete system

$$\psi_\lambda(u(t_i)) - u(t_i+\tau) = 0. \tag{6.1.3}$$

Equation (6.1.3) has 2(2m + 1) equations and 2(2m + 1) + 1 unknowns. We need one more equation. If u(t) = v(t) is an invariant circle, then so is u(t) = v(t+r), for any r. Chan considered 3 ways of getting this last equation.

- to fix one of the components of u at t=0 to some constant c, where

$$min\ u(t) < c \leq max\ v(t).$$

- to seek a circle v(t) that minimizes

$$\int_0^{2\pi} (v(t+r) - \hat{u}(t))^2 dt \tag{6.1.4}$$

over r where $\hat{u}(t)$ is the previous circle that has been computed. Setting the derivative of (6.1.4) with respect to r to zero we get

$$\int_0^{2\pi} (u(t) - \hat{u}(t))^T \hat{u}'(t) dt = 0, \tag{6.1.5}$$

and substituting for u(t) we get

$$\sum_{k=1}^{m} k(\hat{a}_k^T b_k - a_k^T \hat{b}_k) = 0. \tag{6.1.6}$$

- the third is the continuation method.

This method produces a full Jacobian matrix, which has an operation count of order $O(n^3)$ where n is the size of the matrix, and for a modification to this, he used cubic B-splines interpolation instead of the Fourier series. Let

$$P = \{t_i : i = 0, 1...m;\ 0 = t_0 < t_1 < ... < t_m < 2\pi\} \tag{6.1.7}$$

be a partition on $[0, 2\pi)$. Adding $t_{-3}, t_{-2}, t_{-1}, t_{m+1}, t_{m+2}, t_{m+3}$ we can define the normalized cubic B-splines as

$$B_i(t) = (t_{i+4} - t_i)[t_i, ..., t_{i+4}](s - t)^3 for\ \ all\ \ t \in R \tag{6.1.8}$$

The invariant circle can be written as

$$u(t) = \sum_{i=-3}^{m-1} a_i B_i(t) \tag{6.1.9}$$

with u,$a_i \in R^2$, i=-3, -2, -1,...,m-1. Since $B_i(t)$ is identically zero outside the interval $[t_i, t_{i+4}]$, the coefficient a_i is effective only in this interval. Thus the Jacobian matrix of the resulting system has a band structure which therefore reduces the operation count of the system.

For his second method for computing invariant circles, he considered a new form of equation (6.1.2)

$$\psi_\lambda(u(t)) = u(t + \tau) \tag{6.1.10}$$

which can be reduced to

$$\psi_\lambda(u(t)) = u(\sigma(t)), \tag{6.1.11}$$

where

$$\sigma(t) = t + \tau.$$

Equation (6.1.11) ensures that every point remains on the invariant circle after the action of ψ_λ. Using 2m+1 collocation points we get

$$\psi_\lambda(u(t_i)) - u(\sigma_i) = 0 \tag{6.1.12}$$

where $\sigma_i = \sigma(t_i)$ $i = 1, ..., 2m + 1$ with 2(2m+1) equations with 3(2m+1) unknowns. We introduce 2m+1 equations with 1 unknown d as

$$|u(t_i) - u(t_{i-1})|^2 - d^2 = 0 \tag{6.1.13}$$

i = 1, 2, ... 2m+1 thus enforcing the invariant circle corresponding to the time steps to be equally distanced according to the Euclidean norm. The last equation for the unknown d

is given by

$$\int_0^{2\pi} (u(t) - \hat{u}'(t))\hat{u}'dt = 0. \tag{6.1.14}$$

One can represent $u(t)$ by either Fourier series or B-splines, although Chan did not test the method with B-splines.

6.2 Thoulouze Pratt and Jean method

In R^2 the approach can be summarised as follows: Let I be a point in the interior of an invariant Jordan curve γ of the system (1.1.2) and O be a point outside γ. Let x be a point on the half-line IO and compute the iterates $P^i x$ for $i = 1, 2, ...$ If x is on the invariant curve γ and the rotation number is irrational, then there is a first index $i > 1$ such that the line segment $[P^i x, P^{i+1} x]$ cuts the half-line IO (at the point $\lambda(x)$). One then solves

$$x = \lambda(x)$$

for x on IO. The invariant curve can then be computed from the point x. For the details see Thoulouze-Pratt [THP] and [TPJM].

6.3 The method of Spectral Balance

The spectral balance method is a generalization of the harmonic balance method discussed in [PTCL]. In this case the two-periodic solution is a solution of a system with two forcing terms of incommensurate frequencies. The method can be generalized to the case of K incommensurate forcing terms. Consider

$$\dot{x} = f(x) + U_1(t) + U_2(t) \tag{6.3.15}$$

where U_1 and U_2 have ω_1 *and* ω_2 incommensurate frequencies respectively. Let the set of the linear combination of the frequencies be given by

$$A := \{|k_1\omega_1 + k_2\omega_2| : \ k_1, k_2 = 0, \pm 1, ...\}. \tag{6.3.16}$$

Then x(t) is quasi-periodic and does not have Fourier representation but instead has a Fourier Transform $F(x(t))$ which is zero everywhere except on the set A (i.e. at the Fourier frequencies in A). Let $X(k) := Fx(T))$ and let elements in A be given by $\omega_0(=0), \omega_1, \omega_2, ...$ Divide $X(k)$ into three parts: X^0 denotes the $\omega_0 = 0$ coefficient $X(0)$, $X^c(k)$ denotes the vector of cosine coefficients, and $X^s(k)$ denotes the vector of sine coefficients. Thus we can represent x(t) by

$$x(t) = X^0 + \sum_{k=1}^{\infty}\{X^c(k)cos(\omega_k t) + X^s(k)sin(\omega_k t)\}. \tag{6.3.17}$$

This is not the Fourier series because the ω_k are not all harmonics of a single fundamental frequency. Thus the name spectral balance rather than harmonic balance is used. Substituting (6.3.17) into (6.3.15) we get

$$\begin{aligned} 0 &= F^0(X(k)) + U_1^0 + U_2^0 \\ \Omega X^s(k) &= F^c(X(k)) + U_1^c(k) + U_2^c(k) \\ -\Omega X^c(k) &= F^s(X(k)) + U_1^s(k) + U_2^s(k) \end{aligned} \tag{6.3.18}$$

where $\Omega := diag(\omega_1, \omega_2, ...)$, $F := FofoF^{-1}$, $U_1 := F(u_1), and\ U_2 := F(u_2)$.

Truncating the series to K frequencies we get

$$\begin{aligned} 0 &= F_K^0(X_K(k)) + U_{1K}^0 + U_{2K}^0 \\ \Omega_K X_K^s(k) &= F_k^c(X_K(k)) + U_{1K}^c(k) + U_{2K}^c(k) \\ -\Omega X_K^c(k) &= F_K^s(X_K(k)) + U_{1K}^s(k) + U_{2K}^s(k) \end{aligned} \tag{6.3.19}$$

where $\Omega_K := diag(\omega_1, ...\omega_K), and\ F_K := F_K ofo F_K^{-1}$.

Equation (6.3.19) is 2k+1 nonlinear equations in 2k+1 unknowns. If F_K can be evaluated then we can solve (6.3.19) using Newton-Raphson iterations. The F_K can be obtained in the time domain as follows:

- $x_K(t) = F_K^{-1}(X_K(k))$
- $y_k(t) = f(X_K(t))$

- $F_K(X_K) = F_K y_K(t)$

Since x(t) is not periodic, the discrete Fourier Transform cannot be used. Choosing N distinct time points $t_1, ..., t_N$ we get

$$\begin{pmatrix} 1 & a^c_{11} & a^s_{11} & \cdots & a^c_{1K} & a^s_{1K} \\ \vdots & \vdots & \vdots & & \vdots & \vdots \\ 1 & a^c_{N1} & a^s_{N1} & \cdots & a^c_{NK} & a^s_{NK} \end{pmatrix} \begin{pmatrix} X^0_K \\ X^c_K(1) \\ X^s_K(1) \\ \vdots \\ X^c_K(K) \\ X^s_K(K) \end{pmatrix} = \begin{pmatrix} x(t_1) \\ \vdots \\ x(t_N) \end{pmatrix}$$

where $a^c_{jk} := cos(\omega_k t_j)$ *and* $a^s_{jk} := sin(\omega_k t_j)$. We have N equations in 2k+1 unknowns. If N= 2k+1 and the 2k+1 time steps are chosen appropriately, the matrix will be well-conditioned. F_K^{-1} can be obtained by inverting the matrix. The algorithm for choosing the 2k+1 time points that gives nearly orthogonal columns is presented in Kundert et al. [KKSG]. In [USCH], Ushida and Chua choose N>2k+1 evenly-spaced time points with the overdetermined system solved by least-squares. Since this method works for a system with two or more forcing terms with incommensurate frequencies, it is not widely used.

Chapter 7

Conclusion

In this thesis, we have looked at various ways of computing invariant circles and invariant tori. A periodic solution either bifurcates to a period-2 solution through period doubling or bifurcates to an invariant torus through a Hopf bifurcation. Instead of looking at the study of bifurcation of a periodic solution to an invariant torus, we generally look at the corresponding bifurcation of a fixed point to an invariant circle of the associated Poincaré map of the flow.

The method proposed by van Veldhuizen and the pde approach of [DLRR] were described. The method of Van Veldhuizen works for both attracting and repelling circles and the pde approach works for the mixed invariant circles as well. Our main interest here has been to compare the results for these two methods with the Hadamard graph transform method [DLRR2] which we have implemented. The method has proven to be very accurate and efficient in most cases. When the method is applied to the van der Pol equation and the delayed logistic map the results compares nicely with the results of the other two methods. For the coupled oscillators the results seem to differ from that computed by the pde approach and more study of this problem is needed. Future work includes extending the program to higher dimensional maps (for which the standard Poincaré map approach of [VVH1] is apparently not applicable) and to use arc-length parameterization, if r is multi-valued.

Bibliography

[ACHM] Aronson D.G., Chory M.A., Hall G.R. and McGehee R.P. *Bifurcation from an invariant circle for two parameter families of maps of the plane: a computer-assisted study, Comm. Math. Phys., 83, pp. 303-354, 1982.*

[ACS] Arneodo A., Coullet P.H. and Spiegel E.A. *Cascade of period doublings of tori.*

[ADDO] Aronson D.G., Doedel, E.J. and Othmer, H.G. *An analytical and numerical study of the bifurcations in a system of linearly-coupled oscillators, Physica 25D, pp. 20-104, 1987.*

[ADG] Aronson D.G. et al. *Bifurcation from an invariant circle for 2-parameter families of maps of the plane. Commun Math Phys 83, pp. 303-354, 1982.*

[AUB] Aubry *Theory of the Devil's staircase, seminar on the Riemann problem and complete integrability, Ed Chudnovsky, Springer, Lecture Notes in Math, 1978-79.*

[CHA] Chan T.N. *Numerical bifurcation analysis of simple dynamical systems. Masters thesis, Computer Science department, Concordia University, 1983.*

[DLR] Dieci L., Lorenz J. and Russell R.D. *LCCR Decoupling of dynamical systems using boundary value techniques. LCCR Technical Report.*

[DLRR] Dieci L., Lorenz J. and Russell R.D. *Numerical calculation of invariant tori. SIAM J Sci. Stat. Comput. 12, pp. 607-647, 1991.*

[DRL] Devaney R.L. *An introduction to chaotic dynamical systems, Addison-Wesley Publishing Company, Ontario, 1989.*

[GIMC] Gumowski I. and Mira C. *Recurrences and discrete dynamic systems. Lecture Notes in Math. Spring Verlag Berlin-Heidelberg, 809, 1980.*

[GJHP] Guckenheimer J. and Holmes P. *Nonlinear oscillations, dynamical systems and bifurcation of vector fields, Springer Verlag, New York, 1983.*

[HJK] Hale J.K. *Ordinary differential equations. Wiley-Interscience John Wiley and Sons, New York, 1969.*

[IACT] Iooss G., Arneodo, A., Coullet P. and Tresser C. *Simple computation of bicat invariant circles for mappings, Lecture Notes in Math. 898, Springer Verlag, Berlin-Heidelberg-New York, 1981.*

[IOG] Iooss G. *Bifurcation of maps and applications. Math studies, 36, North-Holland, 1979.*

[JEM] Jean M. *Sur la methode des sections pour la recherche de certain solution presque periodique de systemes forces periodiquement. Int Nonlinear Mechanics 15, pp. 367-376, 1980.*

[KASP] Kevrekidis I.G., Aris R., Schmidt L.D. and Pelican S. *Numerical computation of invariant circles of maps. Physica 16D, pp. 243 - 251, 1985.*

[KKSG] Kundert K.S., Sorkin G.B. and Sangiovanni-Vincentelli *Applying harmonic balance to almost-periodic circuits. IEEE Transactions on Microwave Theory and Techniques, MTT-36(2), pp 366-378, February 1988.*

[LEN] Levinson N. *Small periodic perturbations of an autonomous system with a stable orbit. Annals of Math 52, p 727-738, 1950.*

[MAT] Matter *Existence of quasi-periodic orbits for twist homeomorphism of the annular, Topology, 1982.*

[NIN] Nitecki N. *Differentiable dynamics, an introduction to the orbit structure of diffeomorphism, MIT press, 1971.*

[PTCL 15] Parker T.S. and Chua L.O. *Practical numerical algorithms for chaotic systems, Spring-Verlag New York Inc, 1989.*

[THP] Thoulouze -Pratt E. *Existence theorem of an invariant torus of solutions to a periodic differential system. Nonlinear Analysis TMA 5 pp. 195-202, 1981 .*

[TPJM] Thoulouze-Pratt E. and Jean M. *Analyse numerique du comportment d'une solution presque periodique . International Journal Nonlinear Mechanics 17, pp. 319-326, 1982.*

[USCH] Ushida A. and Chua L.O. *Frequency domain analysis of nonlinear circuits driven by multi-tone signals. IEEE Trasactions on Circuits and Systems, CAS-31, pp. 766-778, September 1984.*

[VVH1] Van Veldhuizen M. *A new algorithm for the numerical approximation of an invariant curve, SIAM J Sci. Stat. Comput. 8, pp. 951-962, 1987.*

[VVH2] Van Veldhuizen M. *Convergence results for invariant curve algorithms, Math. Comp. 51, pp. 677-697, 1987.*

[VVH3] Van Veldhuizen M. *On the numerical approximation of the rotation number to appear.*

[VVH4] Van Veldhuizen M. *On the polygonal approximation of an invariant curve. Manuscript.*